Between stress and response: Function and localization of mechanosensitive Ca 2+ channels in herbaceous and perennial plants

Félix Hartmann, Erwan Tinturier, Jean-Louis Julien, Nathalie Leblanc-Fournier

▶ To cite this version:

HAL Id: hal-03385259
https://hal.inrae.fr/hal-03385259v1

Submitted on 19 Oct 2021

Review

Between stress and response: Function and localization of mechanosensitive Ca^{2+} channels in herbaceous and perennial plants

Félix P. Hartmann [1]* , Erwan Tinturier [1] , Jean-Louis Julien [1] and Nathalie Leblanc-Fournier [1]*

[1]   Université Clermont Auvergne, INRAE, PIAF, 63000 Clermont-Ferrand, France

*   Correspondence: felix.hartmann@inrae.fr (FPH), nathalie.leblanc@uca.fr (NLF)

Abstract: Over the past three decades, how plants sense and respond to mechanical stress has become a flourishing field of research. The pivotal role of mechanosensing in organogenesis and acclimation were demonstrated in various plants, and links are emerging between gene regulatory networks and physical forces exerted on tissues. However, how plant cell convert physical signals into chemical signals remains unclear. Numerous studies have focused on the role played by mechanosensitive (MS) calcium ion channels MCA, Piezo and OSCA. To complement these data, we combined data mining and visualization approaches to compare the tissue-specific expression of these genes, taking advantage of recent single-cell RNA-sequencing data obtained in the root apex and the stem of *Arabidopsis* and the *Populus* stem. These analyses raise questions about the relationships between the localization of MS channels and the localization of stress and responses. Such tissue-specific expression studies could help to elucidate the functions of MS channels. Finally, we stress the need for a better understanding of such mechanisms in trees, which are facing mechanical challenges of much higher magnitudes and over much longer time scales than herbaceous plants, and we mention practical applications of plant responsiveness to mechanical stress in agriculture and forestry.

Graphical abstract

Mechanical stresses in tissues are caused by internal pressure and differential growth
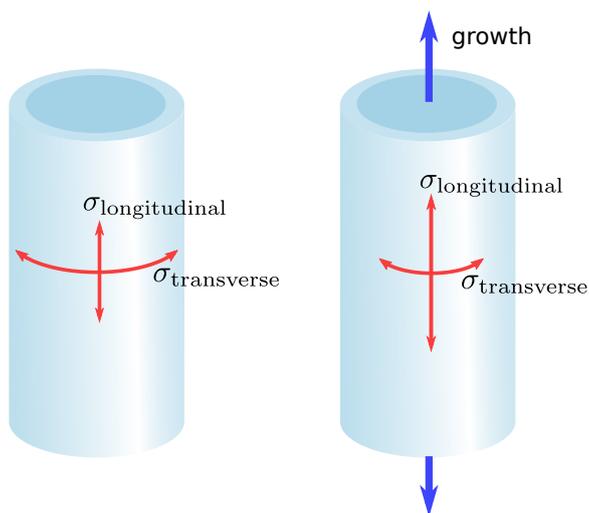
Mechanosensitive Ca^{2+} channel genes have tissue-specific expression levels
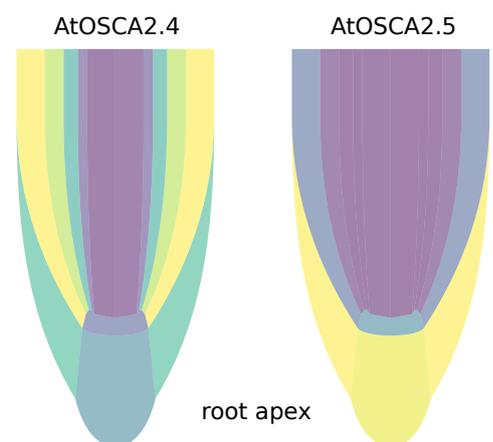
What the localization of stresses and gene expression levels in tissues can tell about the functions of mechanosensitive Ca^{2+} channels in plant development?

1. Mechanical stresses and responses in plants

1.1. Ubiquity of mechanical stress in plants

During their development, plants are exposed to changing and fluctuating mechanical forces, both external and internal [1]. Above ground, transient mechanical loads are caused chiefly by wind [2], but also by rainfall, snow, animals and neighboring plants. Gravity acts permanently, but its magnitude increases with the plant mass and the seasonal bearing of fruits [3], and the lever arm of the weight fluctuates when the plant is swaying in the wind [4] . Under ground, the soil opposes a mechanical resistance to root penetration [5]. In addition, forces exerted above ground are transmitted to the soil, which in turn exerts reaction forces on the roots. Sessile algae and other aquatic plants are supported by buoyancy, which counteracts their weight, but they are dragged by currents [6] or tidal flows [7], and agitated by eddies.

Even in the absence of external forces, plants are mechanically stressed structures [8]. The primary source of intrinsic stress in plants is turgor pressure in cells, which is counterbalanced by stress in the cell wall [9,10]. Within a tissue, a strong stress heterogeneity is possible between neighboring cells [11], due to differences in cell size or shape [12–14], but also cell neighbor number [15].

Because cells are rigidly interconnected through their middle lamella, stress is transmitted from one cell to the other and builds up at the tissue scale [16]. This self-induced stress in the tissues is called "tissue stress" [17], "residual stress" [18], or "autostress" [19] (biologist-friendly definitions of mechanical terms can be found in [20]). Adjacent tissue layers can be subjected to mutual tension due to tissue shape and/or anatomical differences. In the shoot apical meristem (SAM) of tomato, the outer cell wall of the epidermal layer is about seven times thicker than the other cell walls [21]. Being stiffer, the epidermal layer bears much of the load generated by the turgor of the inner tissue and concentrates the stress. This is why the SAM has been described mechanically as a shell under pressure [22,23]. Similarly, the sunflower hypocotyl, where the outer tissue is stiffer and under tension while the inner tissue is compressed, has been described as a cylindrical pressure vessel [24,25]. In these examples, the stress pattern can be predicted based on tissue shape (Figure 1A). In the epidermis of the elongating *Arabidopsis* hypocotyl, however, Verger *et al.* [16] found that the longitudinal stress is higher than the transverse stress, which contradicts the cylindrical pressure vessel model. In this example, the stress pattern is not just based on tissue shape, but predominantly on the anisotropic growth of the inner tissues, which pulls the epidermis in the longitudinal direction (Figure 1B).
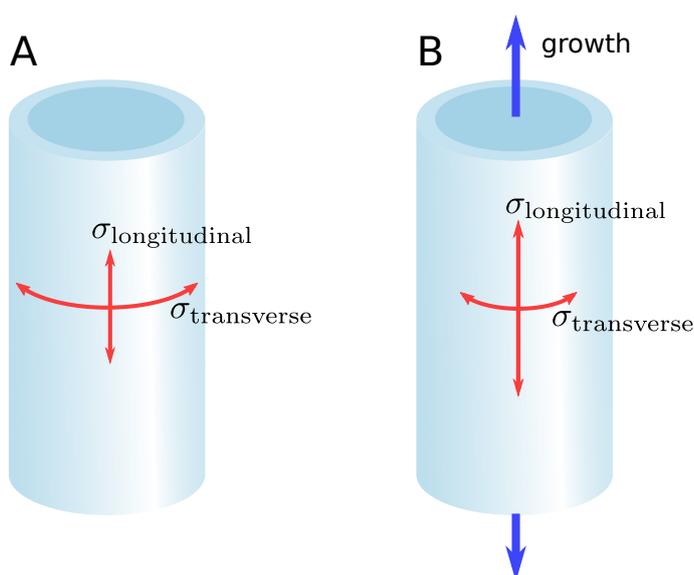
Figure 1. Shape-derived versus growth-derived stress pattern. (**A**) In the pressure vessel model, the stress pattern in the epidermis is determined by the shape of the organ. For a cylindrical organ, the transverse stress is higher than the longitudinal stress. (**B**) Differential growth between the inner tissue and the epidermis can override the stress pattern predicted by the pressure vessel model, leading to a longitudinal stress higher than the transverse stress.

In woody species, additional tissue stress is generated during the maturation of the secondary cell wall [26,27]. These maturation stresses, when they are asymmetric, act as adaptive "plant muscles" in the trunk and branches to control posture and cope with mechanical disturbances [28]. In several tree species, a similar mechanical role is played by the bark, although based on a different mechanism [29].

1.2. Morphogenesis and responses to internal mechanical stress

Turgor pressure is the motor of cell growth, but cell growth induces water influx, which in turn dilutes osmotica in the cell and thus reduces turgor. Therefore, sustaining the osmohydraulic motor requires a constant adjustment of osmoticum concentration. This adjustment is thought to involve some sensing of the mechanical state of the cell wall (its thickness, strain, or stress) and a feedback mechanism on osmoticum influx and efflux [30].

Apart from sustaining cell turgor, responses to mechanical stress are ubiquitous in plant morphogenesis. A mechanical instability can be the trigger of a reaction cascade leading to a final shape, for instance the formation of lobes in epidermal pavement cells [31]. Cell pressurization generates hotspots of compressive stress in the anticlinal walls, which can cause sudden and localized bendings of the wall, a phenomenon termed "buckling". The small displacement caused by the buckling is then amplified by a positive-feedback mechanism involving the cortical microtubules, until a lobe is formed [31]. The global effect of lobe formation in pavement cells is to keep mechanical stresses low [13]. Could buckling also initiate leaf primordia in the SAM? Many experimental and numerical results suggest instead that outgrowths at the meristem surface follow local maxima of the plant hormone auxin [32–35]. Auxin loosens the cell wall and facilitates organ emergence [36]. However, the polarity of the auxin transporters PIN is influenced by mechanical perturbations, creating a feedback loop between auxin distribution and mechanical stress [37,38]. The outgrowth of a primordium compresses the surrounding tissues. This does not usually cause buckling, but induces the expression of the homeobox gene *SHOOT MERISTEMLESS* (*STM*), which marks the boundary domain around primordia and ensures organ separation [39]. *STM* expression is quantitatively correlated to curvature in the boundary domain, which is itself a proxy for mechanical stress. The mechanotransduction pathway leading to *STM* expression has been proven to be auxin-independent [39].

The molecular actors through which mechanical stress activates *STM* are not known. In many instances, mechanics-driven morphogenesis involves a reorientation of microtubules in response to mechanical stress [22,40,41]. In the periphery of the SAM, microtubules are perpendicular to the direction of maximal strain, whereas they are parallel to the direction of maximal strain in the boundary between the primordium and the meristem [42]. This shows that while the response of microtubules to mechanical stress or strain is not completely clear, they are central actors in mechanosensing, including shape sensing [43]. Based on *in vitro* experiments [44] and *in silico* simulations [45], Hamant *et al.* [46] hypothesized that microtubules are sensors of tensile stress direction, or at least sensors of changes in tensile stress direction. Microtubules guide the deposition of cellulose microfibrils on the cell wall [47], thereby increasing locally its resistance to tension and changing globally the pattern of stress distribution in a tissue. This is how a mechanical feedback loop could arise and help organs to reach their final shape in a robust way, as neatly exemplified in the sepal by Hervieux *et al.* [48,49].

1.3. Thigmomorphogenesis and responses to external stress

While internal mechanical stresses play a key role in driving organogenesis until a determinate target shape is reached, external stresses are inherently unpredictable and a source of dangerous perturbations. Plants face these challenges through an adaptive development relying on appropriate responses. This is especially true for perennial plants, which experience vast changes in size and mass through their life stages, and hence large variations in external mechanical stress. Adaptation occurs mainly in terms of growth, that is addition of material, quantitatively and qualitatively. In trees subjected to transient bendings, the root biomass increases and the root architecture changes in a way that improves anchorage [50,51]. The same treatment, mimicking the effect of wind, induces a reduced height growth and an increased diameter growth in *Ulmus americana* [52] and *Prunus avium* [53], with an ovalization of the stem cross-section along the bending direction. In poplar, the inhibition of height growth is less significant, but an ovalization has also been observed [54]. This geometrical change improves the mechanical safety margin of treated trees [54]. Qualitatively, imposed bendings modulate

wood differentiation. In *Abies fraseri*, the tracheids formed under bidirectional bending treatment have smaller lumens than in normal wood and higher microfibril angle [55]. Although bending-induced wood shares some similarities with compression wood, it has a distinctive anatomical structure and has been termed "flexure wood" by Telewski [55]. In poplar, transient unidirectional bendings cause a decrease in vessel frequency and an increase in the thickness of secondary cell wall of fibres [56]. Unlike bidirectional bendings, unidirectional bendings allow the observation of differential effects between the stretched and compressed sides of the bent stem. For instance, vessel size is decreased in the stretched side only [56]. Thus, while radial growth depends on the absolute magnitude of strains, wood-forming tissues have the ability to distinguish between positive and negative strains. Overall, wood produced under mechanical stress is more resistant to damage and enhances the bending strength of the stem [57].

These various manifestations of growth acclimation to mechanical perturbations are collectively termed "thigmomorphogenesis" [58]. Thigmomorphogenesis tends toward better self-support and increased resistance of trees to wind [59]. Despite its high cost in terms of biomass allocation, it is a priority requirement for trees, even under severe water stress [54]. Tree acclimation to wind loads has been demonstrated not only in controlled experiments, but also in a forest context [60]. Although most striking in perennials, thigmomorphogenesis has been also reported in herbaceous plants, for instance *Arabidopsis* [61,62] and *Plantago major* [63], and aquatic plants [64].

1.4. Localized versus distant responses

Mechanical actions can be very localized, and initiate equally localized responses. For example, the emergence of a lateral root can be a response to a local bending [65,66]. Lateral root emergence is also an example of mechanical stress exerted from inside. The lateral root can emerge only if the epidermis yields to internal pressure. This is mediated by a complex signaling cascade which modulates the mechanical properties of cell walls [67]. External stresses are exerted by the soil on the progressing root cap. When a poplar root encounters a physical obstacle, its growth rate sharply decreases, even before the force builds up at the contact point [68]. This early growth response is most likely induced by the mechanosensing of very small forces on the root cap. In laboratory conditions, when the root is growing in a nutrient solution and is free to move laterally, the force exerted on the obstacle increases progressively until the root buckles [68]. If the root is laterally supported, like in a natural environment, it can reach an axial force much larger than the buckling threshold [68].

To investigate the ability of *Arabidopsis* roots to progress in a medium with varying strength, Roué *et al*. [69] designed an experimental setup consisting of two layers of growth medium containing Phytagel at different concentrations. The lower layer has a higher concentration and is consequently more resistant to penetration, mimicking a more compact soil layer. Upon contact with the interface between the two layers, the root either penetrates the lower layer or reorients its growth [69]. *Arabidopsis* genotypes exhibiting contrasted root cap morphologies have different penetration abilities. The *fez-2* loss-of-function mutant, with a pointed cap, penetrates less often the denser layer than the Col-0 wild type, which in turn has a lower penetration ability than the *smb-3* loss-of-function mutant, with a rectangular-shaped cap [69]. It is yet to be determined whether these unequal penetration abilities are caused solely by differences in root cap morphology, or results from possible mutation-induced alterations of the mechanical rigidity or mechanosensitivity of the root cap. Non-penetrating roots of all three genotypes undergo a rapid curving interpreted as passive buckling. In some cases, especially when the change in medium strength across the interface is highest, the buckling deviates the root apex in the horizontal direction and, later, a second curving reorients the apex to the vertical. This second curving is interpreted as an active movement resulting from the interaction between gravitropic and thigmotropic response [69].

Responses can also occur far away from the stimuli. In manually bent tomato plants, although only the basal part of the stem directly experiences a mechanical stress, a growth response is also observed in distant primary meristems in the form of reduced height growth [70]. Since the estimated velocity of this long-distance signaling is incompatible with hormone transport [71], it is either hydraulic [72,73] or electrical [74] in nature. In *Arabidopsis*, long-distance signaling is also observed after mechanical wounding [75]. Tissues far from the wound rapidly synthesize jasmonates, which have been proven to enhance pest resistance and regulate growth [76]. Farmer *et al*. [77] hypothesized that the hydraulic

and electrical signals induced by a wound could be mechanically coupled. After wounding, a traveling pressure wave increases locally and abruptly turgor in xylem vessels, which in turn exert strong pressure on adjacent cells. According to the so-called "squeeze cell hypothesis", mechanical stress in squeezed adjacent cells activates Ca^{2+} channels, causing ion fluxes which propagate from cell to cell.

In poplars, local flame wounding on the stem alters stem elongation and stimulates, in stem apices, the expression of *JAZ5*, a gene encoding Jasmonate-ZIM domain protein [78]. On the other hand, moderate poplar stem bending does not trigger any remote response [78] although it induces a long-distance electrical signal [74]. A possible explanation could be that a moderate bending does not cause a wound, and therefore induces a weaker signal, which attenuates over a shorter distance [74]. This would also explain why tomato plants, which are short, display a remote growth response to bending [70], whereas in bent poplar the electrical signal cannot travel the longer distance between the wounding point and the stem apex.

As a conclusion, plants respond to mechanical stress in many different ways. However, responding to a stress is only possible if the stress is perceived. Mechanosensing and mechanotransduction have hence been the focus of numerous studies using the powerful tools of molecular biology. The two next sections of this review will be devoted to the description of some molecular actors of mechanosensing and how they can be related to the growth and development of roots and stems.

2. Mechanosensitive channels across the Planta kingdom

2.1. Diversity of mechanosensing mechanisms

As described in the previous section, cells from diverse tissues detect mechanical signals through potentially diverse mechanisms, triggering different biological responses. These different types of mechanical stresses (e.g.. bending, dryness or hyperosmotic shock) cause stretching of the plasma membrane, displacement of the plasma membrane relative to the cell wall (e.g. cell-wall loosening during cell expansion, hypo-osmotic shock), changes in the orientation of cortical microtubules [22] and could also affect the nucleus through interactions between cellular compartments via the cytoskeleton [79]. The perception of a mechanical stress by a cell is a rapid process requiring a quick conversion of a mechanical signal into a biological signal. Major progress has been made in recent years in identifying the molecular players involved in mechanosensing. Two major types of candidates emerge from these studies: (i) receptor-like kinases from *Catharanthus roseus* RLK1-like subfamily (CrRLK1) identified in approaches aimed at studying the maintenance of cell wall integrity (see review by Bacete and Hamman [80] and references therein), and (ii) mechanosensitive (MS) ion channels (see review by Frachisse *et al*. [81] and references therein).

Among the CrRLK1 family, FERONIA is a player at the interface of many responses involving the perception of mechanical stresses. Thus, besides its well-known role in cell growth and hormone signaling [82], *fer* loss-of-function mutant has impaired ion signaling, reduced expression of mechanoresponsive genes and altered root growth responses to mechanically challenging environments when exposed to local touch or bending stimulation [83]. Furthermore, FERONIA also appears to play a role in developmental responses involving the perception of mechanical stimuli such as root nutation [84], root gravitropism [85], roots encountering an impenetrable cover glass barrier [83]. This transmembrane protein has an extracellular domain containing two MALECTIN-like domains that may be involved in binding to cell wall components and an intracellular kinase domain that may trigger phosphorylation-dependent signaling pathways during mechanotransduction. Interestingly, a recent work shows the involvement of several phosphoproteins—MAP kinase kinase (MKK) and a novel protein named TREPH1—in the process of the most-studied thigmomorphogenetic response in *Arabidopsis*, i.e. the emergence of the flowering stem [86].

The other important actors are the MS channels, which are inserted in the membrane and function as ion transporters across the membrane when under mechanical stress. They are prime candidates for converting a mechanical signal into a chemical signal. Described in various reviews [81,87,88], several types of MS channels have been identified in plants, including the anion-permeable channel MSL and several types of calcium-permeable channels families like MCA, Piezo and OSCA.

Another way to understand the early stages of mechanosensing is to follow the dynamics of intracellular calcium concentrations. Indeed, calcium cations are typically involved as quick secondary messengers in numerous plant responses [89]. A rapid increase in concentration of cytosolic Ca^{2+}

ions occurs in response to mechanical stimuli like touch, wind or osmotic variations in plants [90–93], triggering a specific local response, but also possibly causing distant responses by propagating electrical signals [94,95]. The diversity of calcium signatures depending on the nature of the mechanical stimuli is very well described in the study carried out by Monshausen *et al.* [67] on the *Arabidopsis* root. In this study, the authors showed that touch, bending or root growth against an impenetrable barrier trigger a rapid (< 30 sec) increase in intracellular calcium. However, the calcium signatures are different in duration and in the peak intensity, suggesting the potential involvement of different mechanosensing mechanisms or the importance of a sensitivity threshold. It is also important to note that, in the case of bending stimulus, the calcium increase is visible mainly in the tensile tissues of the root, suggesting potentially different sensing mechanisms between compressive and tensile strains. Moreover, the calcium response is biphasic, involving two peaks of different intensities. The channels involved in this calcium response have not been identified to date. However, FERONIA seems to be involved in this response since *fer* loss-of-function mutants subjected to such mechanical stimulation do not show the second calcium peak, characteristic of this biphasic response. However, the calcium-permeable channels responsible for the first calcium peak and the role of FERONIA in triggering the second calcium peak remain to be identified. Shih *et al.* [83] report that under their conditions, the loss-of-function mutant *mca1* and the quintuple mutant *msl4 msl5 msl6 msl9 msl10* are not impaired in this response.

Given the predominant position of the calcium-permeable channels in the literature on plant mechanotransduction, we will focus in the rest of this section on this mechanosensing mechanism. It should also be noted that the genes involved in the calcium signaling pathway such as calmodulins were among the first genes discovered to be regulated at the transcriptional level by mechanical stimuli [96].

2.2. Description and functioning of mechanosensitive Ca^{2+} channels

2.2.1. The Mid1-Complementing Activity (MCA) family

The MCA family was first described in *Arabidopsis thaliana* [97]. *AtMCA1* and *AtMCA2* are paralogs, with high sequence homology (the relationships between gene names and accession numbers are given in Table S1).

The MCA channel was thought to be organized as a homotetramer with a small transmembrane region forming the pore (with only one transmembrane domain per monomer) and a larger cytoplasmic region of motifs (an EF hand-like motif, a coiled-coil motif and a cysteine-rich region homologous to the PLAC8 or DUF614 motif near the carboxyl terminus) regulating the pore [98–100]. While the PLAC8 domain is observed in eukaryotic proteins, its combination with the transmembrane domain and the EF hand-like motif is specific to streptophytes, and absent in chlorophytes (Figure 2A). Therefore, in contrast to other MS channels (Figure 2), MCA appears to be specific to land plants [101]. This may relate to the specific selective pressure faced by land plants, which can not rely on water buoyancy to support themselves and hence developed posture control mechanisms to maintain an erect habit [4]. However, it is not known whether *MCA* genes are directly involved in posture control.

Even if a fine analysis of the electrophysiological properties of this MS channel is lacking, *MCA1*-expressing *Xenopus laevis* oocytes enhances ionic currents following mechanical stimuli such as hypo-osmotic shock or in response to negative pressure in the patch pipette [97,102]. *In vivo*, AtMCA1 appears to be involved in Ca^{2+} uptake in *Arabidopsis thaliana* roots [103]. It is also thought to be crucial in the process of root penetration in a hard agar medium [97]. Indeed, using a two-phase agar method, Nakagawa *et al.* [97] demonstrated that the primary roots of *mca1*-null plants fail to penetrate a harder agar medium from a softer one, whereas *mca2*-null seedlings are able to grow like wild-type (WT) plants depending on the hardness of agar medium [103].

Hypergravity has the effect of inhibiting the growth of the hypocotyl of *Arabidopsis thaliana*. This effect is reduced in an *mca*-null mutant compared to WT, and is enhanced in an *MCA*-overexpressing mutant [104]. These results also suggest the involvement of MCA in gravity perception.

2.2.2. The Piezo family

First identified in vertebrates, the mechanically-activated Piezo family (Figure 2B) is conserved with homologs in prokaryotes, plants, and invertebrates [105].
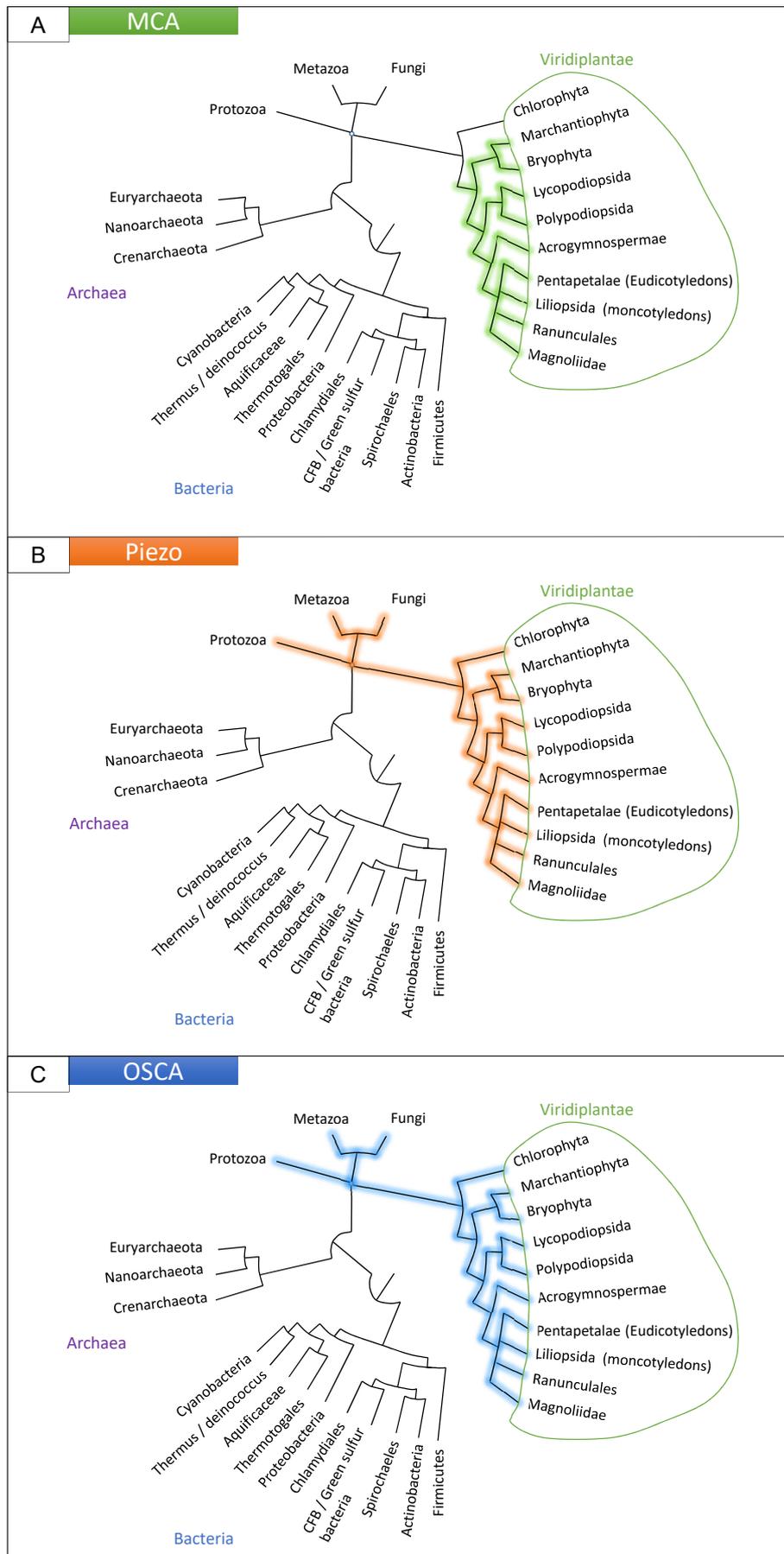
Figure 2. Presence of the *MCA* (A), *Piezo* (B) and *OSCA* (C) families in the tree of life. See Appendix A for details.

In vertebrates, Piezo 1 and 2 are large structures of approximately 2500 amino-acids including many transmembrane regions. Cryo-electron microscopy (cryo-EM) studies have shown that Piezo1 possesses a tree-bladed, homotrimeric structure comprising a central ion-conducting pore module [106–109]. Each peripheral blades has 38 transmembrane regions, with the peripheral blade-like structures on the extracellular side and three beams on the intracellular side. With its distal blades and the central pore, the Piezo1 channel could have a lever-like mechanotransduction mechanism that could explain how it converts mechanical forces into a cation influx (see the illustrated model proposed in [110]).

In vertebrates, Piezo 1 and 2 are mechanotransducers able to convert a mechanical force into an increase in cytosolic Ca^{2+}, enhancing various Ca^{2+}-dependent downstream signaling pathways. Piezo1 can be activated by a large variety of mechanical stimulation like poking, stretching or any local membrane tension, while Piezo2 seems to be strongly activated only by poking. In *Arabidopsis*, Mousavi *et al*. [111] studied the electrophysiological properties of the unique Piezo protein via a chimeric PZO1 construct including the C-terminal part of AtPiezo1 (containing the putative pore region) and the N-terminal part of the mouse mPiezo1 to allow the anchoring of the protein in the plasma membrane. They showed that this chimeric PZO1 protein is functional and acts as a MS channel when expressed in naive mammalian cells.

Piezo ion channels play key roles in mechanobiological processes in animals, for example in vascular development or touch sensing [112]. In plants, their role is still largely unknown, with only four studies to date. In *Arabidopsis thaliana*, AtPiezo is a key element of the immune response to the cucumber mosaic virus and the turnip mosaic virus [113]. In addition, several recent works have made major advances on the potential role of AtPiezo in *Arabidopsis* root growth in responses to substrate impedance [111,114]. When *atpiezo* null-mutant plants were grown *in vitro* in vertical plates leading to root growth on the surface of the medium, no difference was observed from WT plants [114]. However, when the plants were grown in a horizontally placed plate with 0.8% agar, the root ability to penetrate the medium decreased by about 20% compared to WT. Similar results were obtained by Mousavi *et al*. [111], who showed that when seedling roots grew within the Murashige and Skoog medium, the length of the mutant roots were shorter compared to WT. Both studies suggest a direct role of AtPiezo in mechanosensing in roots. Interestingly, as detected for Atmca1 [103], in these two studies, reporter gene expression of Piezo::GUS in transgenic *Arabidopsis thaliana* plants showed that *AtPiezo* is mainly expressed in the root cap in a cross-section of the root tip.

However, in moss (*Physcomitrium patens*), PpPiezo1 and 2 are localized in the tonoplast and are thought to be involved in the regulation of vacuole shape in apical caulonemal cells [115]. These results raise the question of the role of the vacuole in mechanosensing. A study linking cellular elongation, vacuole expansion and the role of FERONIA has been carried out by Dünser *et al*. [116]. Using epidermal atrichoblast root cells and by combining different fluorescent dyes in cellular compartments, they showed that the cytosol shows relatively minor volume expansion during epidermal elongation compared to the relative increase in vacuolar size. By using different approaches, they investigated the possibility that apoplast acidification/cell wall loosening is sensed and provides a feedback control for vacuolar morphogenesis. Again, *fer* loss-of-function mutant vacuoles were markedly less affected by extracellular constraints of the substrate suggesting a role of a FER-dependent signaling in regulating intracellular expansion of the vacuole. It would be interesting to analyze if Piezo could be involved in these mechanisms.

2.2.3. The OSCA family, hyperosmolarity-gated calcium-permeable channels

OSCA is the largest family of mechanically-activated ion channels identified and conserved across eukaryotes, including fungi, animals (homologous TMEM63 channels) and plants (Figure 2C) [117,118]. In *Arabidopsis thaliana* and *Populus trichocarpa*, OSCA is composed of 15 and 17 genes respectively, separated in four clades (Figure 3). Murthy *et al*. [118] tested the mechanosensitivity of channels across clades by selecting one gene from each clade in *Arabidopsis thaliana*. Electrophysiological results suggest that the channels encoded by the three genes *AtOSCA1.8*, *AtOSCA2.3*, and *AtOSCA3.1* are mechanosensitive, a trait that would not be found for the AtOSCA4.1 channel (Murthy et al., 2018). Clade 4 shares the least homology with clade 1 (Figure 3). AtOSCA4.1 may have a distinct function.

Cryo-EM studies revealed a molecular structure formed by a homodimer with two pores [119–121]. Work on AtOSCA1.1 and AtOSCA1.2 suggests that the resulting pores are non-selectively permeable
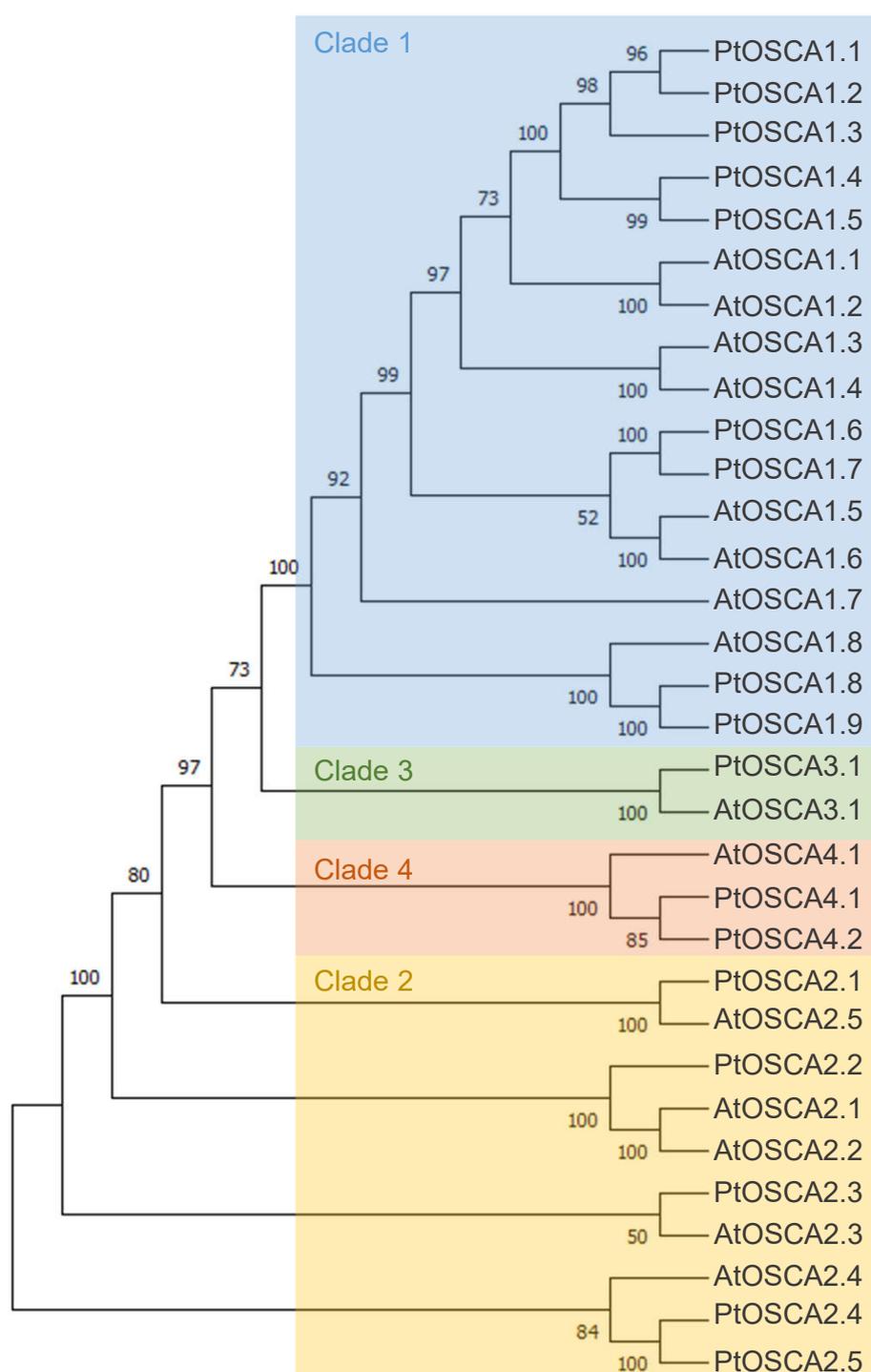
Figure 3. Maximum-likelihood phylogenetic tree of OSCA of *Arabidopsis thaliana* and *Populus trichocarpa*. The percentage of tree in which the associated taxa clustered together is shown next to the branches. Initial trees for the heuristic search were obtained automatically by applying Neighbor-Join and BioNJ algorithms to a matrix of pairwise distances estimated using the JTT model, and then selecting the topology with superior log-likelihood value. The tree is drawn to scale, with branch lengths measured in number of substitutions per site. This analysis involved 22 amino acid sequences. All positions with less than 50% site coverage were eliminated, i.e. fewer than 50% alignment gaps, missing data, and ambiguous bases were allowed at any position (partial deletion option). There were a total of 770 positions in the final dataset. Evolutionary analyses were conducted in MEGA X .The four clades are colored: blue (Clade 1), yellow (Clade 2), green (Clade 3), and orange (Clade 4).

to cations [118]. Each subunit is composed of 11 transmembrane domains, as well as a soluble cytosolic domain with an RNA recognition motif. The cytosolic domain has a distinct structural feature in the form of extended intracellular helical arms parallel to the plasma membrane. These arms are well positioned to detect a change in the lateral tension of the inner lipid bilayer sheet caused by a change in turgor pressure [122]. Membrane topology appears to be conserved across eukaryotes [118].

The physiological functions of OSCA channels remain poorly understood. Until now, several studies have implicated the *OSCA* genes in osmotic responses. However, a hypo- or hyper-osmotic shock results in a stretching or a relaxation of the plasma membrane, and can be considered as a mechanical stimulation. AtOSCA1.1 mediates osmotic signaling in guard cells and roots cells, and attenuates water transpiration and root growth in response to osmotic stress [123]. AtOSCA1.3 controls plant stomatal immunity [124]. In maize, ZmOSCA2.4 has been shown to be involved in drought tolerance in transgenic *Arabidopsis* [125]. Recently, an RNA-seq study by Procko *et al*. [126] suggested an involvement of the MS channels MSL and OSCA in triggering the touch-sensitive hair of the Venus flytrap (*Dionaea muscipula*). It would be interesting to see whether OSCA channels have a role in other mechanical processes.

The diversity of calcium-permeable MS channels present in plants could explain what makes a mechanically-induced $[Ca^{2+}]_{cyt}$ signaling pattern specific (Ca^{2+} footprint), leading ultimately to a specific, graded physiological response. As very well explained in a recent review by Frachisse *et al*. [81], the detailed characterization of the electrophysiological properties of these different channels shows that they differ in their permeation and gating properties (activation threshold, conductance, inactivation). They can therefore trigger distinct signaling pathways and potentially be activated differentially, depending on the magnitude of the mechanical stress.

3. Mechanosensitive channels in tissues and organs

The functions of the different families of MS channels are far from being fully understood. Several questions remain to be answered regarding their role during either development or acclimation to external mechanical stress. Are there relationships between the localization of MS channel and the localization of stress and responses? Is the number of different types of these channels in a membrane responsible for a difference in the sensitivity of cells to membrane stretch? Within a multigene family, is there redundancy between proteins or are they specifically localized in tissues? Do these different channels interact in the same signalization pathways? In relation to these questions, the most-studied family of MS channels is the anion-preferring MSL family [88]. Within this MSL family, consisting of 10 members in *Arabidopsis*, some isoforms localize in membranes of different cell compartments (plasma membrane, tonoplast, mitochondrial membrane) and are expressed in a tissue-specific manner. Concerning calcium-permeable channels, MCA and OSCA channels are located in the plasma membrane [97,123], whereas Piezo1 is located in the tonoplast [115]. However, information is incomplete regarding the location of their expression.

Studying the regulation and the localization of the expression of these genes could help to design new hypotheses on their function. In this section, through data mining and visualization, we compare the tissue-specific expression of these three families of MS channels in plants, focusing on root and stem tissues. In *Arabidopsis*, recent studies using RNA-seq approaches carried out on single cells have revealed the expression of thousands of genes in different root tissues [127] or in tissues of the floral stem [128]. We also studied the expression profiles of members of these families in poplar using RNA-seq data obtained by Sundell *et al*. [129] from laser dissection of stems comprising developing phloem and secondary xylem.

3.1. Mechanosensitive channel expression in the root tip

As root cap cells are the first to encounter obstacles, this tissue is a potential mechanosensing site. Therefore, the molecular mechanisms underlying root-obstacle avoidance has been the subject of much research in recent years. To mimic the progression of the root in the face of mechanical stresses related to soil impedance, studies were conducted using several *in vitro* systems: artificial root barrier systems or experimental setups consisting of two layers of growth medium containing Phytagel at different concentrations to modify the physical strength of the medium [69]. The typical responses of roots encountering an obstacle are a reduction of root growth and a resulting "step-like" growth pattern,

with only the root tip remaining in contact with the barrier surface. By RNA-seq approaches performed on whole roots of *Arabidopsis* seedlings collected either 6 h or 30 h after barrier contact, combined with reporter line and mutant studies, Jacobsen *et al*. [130] showed significant changes in reactive oxygen species (ROS), ethylene and auxin signaling pathways, confirming several previous studies. In particular, they demonstrated that when ethylene signaling is perturbed in ethylene-insensitive mutants, the root growth is less inhibited than in WT after barrier contact. In the same way, auxin transport effects were observed through altered bending responses, which is consistent with other studies using PIN-mutants, pharmacological assays and image analysis [131].

Meanwhile, in the last fifteen years, several studies have evidenced the role of MS channels in root responses to mechanical impedance stress. However, tissue-specific mecanosensing and the role of the different MS channels are far from being well-understood. So far, no link between the activation of auxin, ROS and ethylene signaling pathways and the activation of MS channels have been demonstrated during the root response to substrate impedance. Furthermore, *in vivo* root growth dynamics and root trajectory following the contact of the root apex have not been finely analyzed in *mca*-mutants or *piezo*-mutant of *Arabidopsis thaliana*. Using different root-cap development mutants, this type of approach has shown that the shape of the root cap and the growth rate of the root are parameters that strongly influence the mechanical resistance of the root to buckling or the magnitude of the force applied by the root on the substrate [69]. If such anatomical or growth defects were found in these mutants, these parameters could influence the ability of *Arabidopsis* roots to progress in a medium with varying strength. In addition, the growth arrest observed following contact of the root with the substrate suggests a change in cell elongation, at a distance from the contact point, in the elongation zone. How is the signal transmitted? Are the innermost cells deformed and respond to this mechanical stress? Could the *OSCA* genes play a role in this response?

To study the location of the expression of these different genes in different cell types of the root, we compared their tissue-specific expression using novel visualizations of data obtained by Ryu *et al*. [127] with single-cell RNA-seq method.

When using a common scale to compare the expression levels of all tested genes (Figure A1), it appears clearly that *AtOSCA2.4* and *AtOSCA3.1* reach the highest level of expression in the tissues composing the root. While *AtOSCA2.4* is most highly expressed in the outermost tissues (epidermis, cortex, lateral cap and columella), *AtOSCA3.1* expression is high in the phloem and cortex and at a lower level in the columella and epidermis. The genes *AtMCA2*, *AtOSCA1.4*, *AtOSCA1.5*, *AtOSCA1.6*, *AtOSCA1.7*, *AtOSCA2.5*, *AtOSCA4.1* and *AtPiezo* show a 10-fold lower expression level than the other genes. However, when the expression levels of these genes are plotted on a scale specific to each gene (Figure 4), very distinct expression profiles emerge. For example, *AtOSCA2.5* appears to be expressed in cap tissues, *AtOSCA1.5* in the pericycle, *AtOSCA1.7* in the phloem, *AtMCA2* in the endodermis and *AtOSCA1.4* in epidermal cells developing a root hair. Although low, the tissues with the highest amount of *AtPiezo* transcripts are the cortex, lateral cap, and xylem. These data are in agreement with the histochemical approaches using the GUS reporter gene highlighted by Mousavi *et al*. [111], although this transcriptomic approach, which allows a stronger differentiation of expression levels, shows that *AtPiezo* expression in the columella is relatively low. Similarly, the tissue-specific expression of *AtMCA1* in the columella and xylem was revealed by Yamanaka *et al*. [103]. Regarding the vascular tissues of the stem, apart from *AtOSCA2.1*, the genes of the *OSCA* family show a higher expression in the phloem in contrast to *AtMCA1* and *AtPiezo*. Concerning the *OSCA* gene family, it is interesting to observe that genes that are very close in sequence and probably originate from the same duplication event (see the phylogenetic tree Figure 3) can present very different expression profiles (e.g. *AtOSCA1.1* and *AtOSCA1.2*, or *AtOSCA2.1* and *AtOSCA2.2*). These results suggest that these proteins may be involved in different physiological functions. The expression of many *OSCA* genes in the lateral cap or columella (*AtOSCA1.1*, *AtOSCA1.3*, *AtOSCA2.3*, *AtOSCA2.5*) could encourage studies on their role in root penetration or in the perception of water stress at the root level. In the context of mechanosensing, it would also be interesting to study *AtOSCA2.4* and *AtOSCA1.4*, which show, respectively, strong and specific expression in rapidly-expanding epidermal cells. In contrast, the expression level of all these genes encoding MS channels is very low in the meristematic zone.
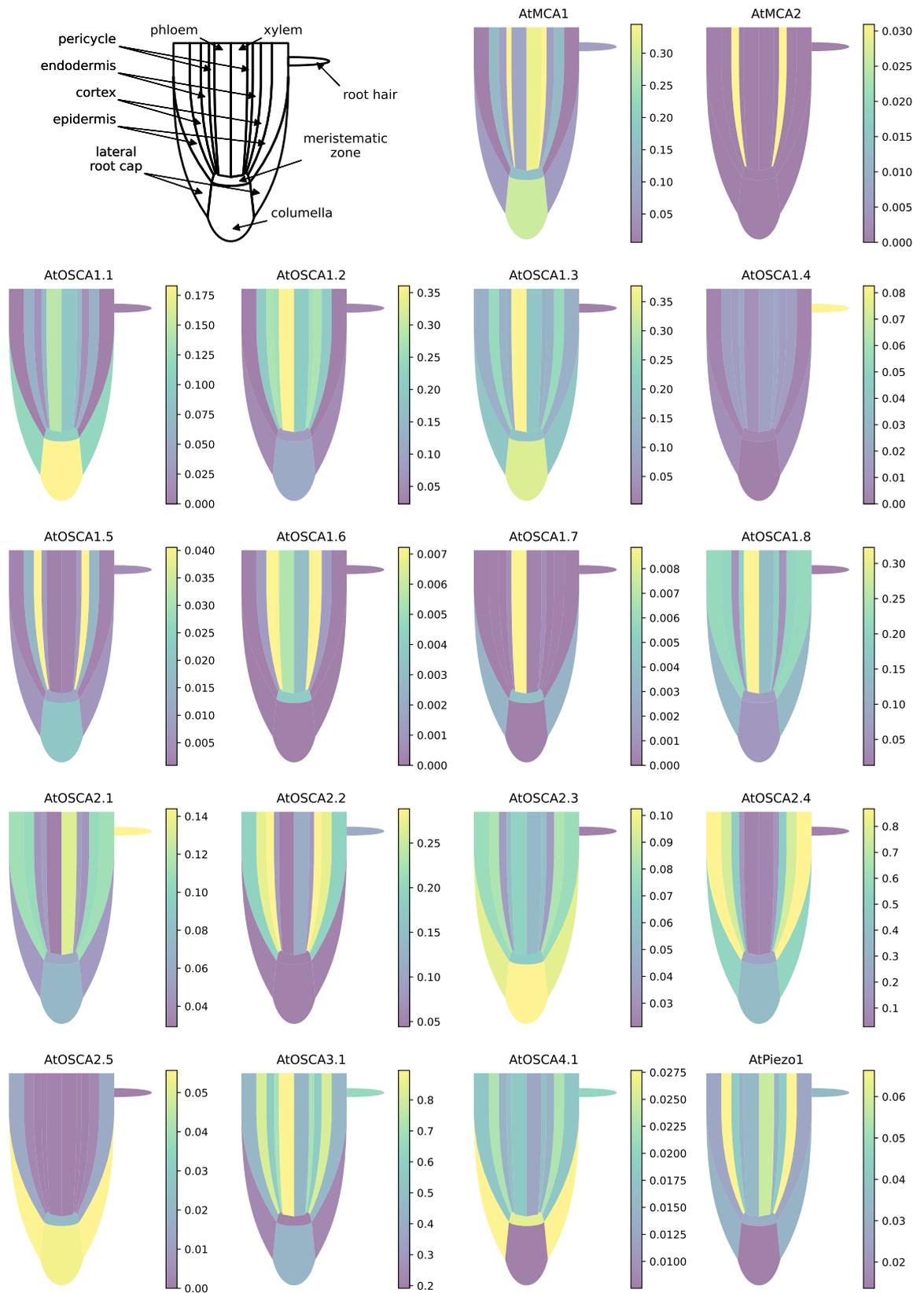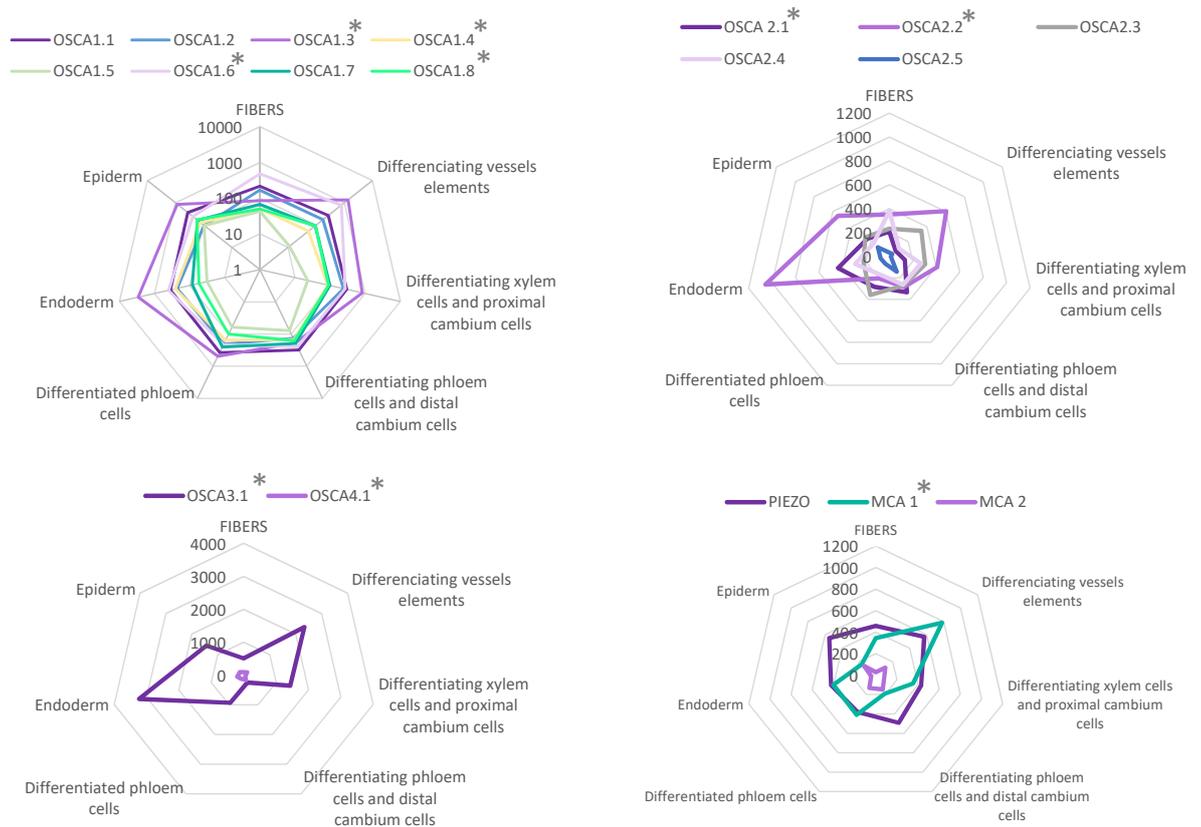
Figure 4. Expression patterns of *MCA*, *Piezo* and *OSCA* genes in different tissues of the *Arabidopsis* root. Data for each gene were retrieved from the BAR ePlantArabidospsis website (https://bar.utoronto.ca/eplant). To facilitate the graphical representation of expression levels in tissues, only expression values from sub-clusters containing differentiated (not differentiating) cells were used. In the stele, only the expression data from xylem- and phloem-cell types are shown. In the meristematic zone, we represented the expression mean of dividing cells and cells from the quiescent center. See Appendix B.1 for details and Table S1 for the relationships between gene names and accession numbers.

3.2. Mechanosensitive channels expression in the stem

Like in the root, cells in the plant stem are sensitive to external mechanical stress during primary or secondary growth. Numerous studies showed that repeated bending of the stem triggers an increase in stem diameter growth and anatomical changes in internal stem tissues, affecting especially the development of secondary tissues [55,56,61]. However, studying the spatio-temporal responses *in vivo* in the tissues of a secondary-growing stem is complex and molecular studies seeking to reveal the mechanisms underlying this acclimation response to external mechanical stimuli are underdeveloped. In poplar, Pomiès *et al*. [132] showed that the stem transcriptome is massively remodeled in response to a single transient-bending stimulus. 2663 genes, representing 6% of the genome, were found to be regulated after bending, with a large proportion (75%) of these genes being regulated within the first 2 h after bending. Short-term transcriptomic responses entailed a rapid stimulation of plant defense and abiotic stress signaling pathways, including ethylene and jasmonic acid signaling [132]. Late transcriptomic responses affected genes involved in cell wall organization and/or wood development. By studying more specifically the stretched and compressed zones of the bent stem, Roignant *et al*. [56] demonstrated that some genes (e.g. *MYB69* transcription factor, microtubule-associated protein encoding gene *MAP70*) were regulated in the same way in both zones, while *FLA* genes, encoding fasciclin-like arabinogalactan proteins known to accumulate during tension wood formation, were specifically expressed in the stretched zone. These data suggest that cells sense differentially stretch and compression induced by stem bending. To date, the role of MS channels in this type of response has not been studied. However, the growth and anatomical differences that have been established show that this sensitivity to bending modifies the cambial activity within the stem. Are all living cells in the stem mechanosensitive or is the sensing localized, and secondary signals are transmitted remotely to the cambium?

As in the case of the root, we took advantage of recent RNA-seq data on single cells or isolated tissues to compare the expression of the *MCA*, *Piezo* and *OSCA* genes. As shown in Figure 5, *AtOSCA4.1*, *AtOSCA2.5* and *AtMCA2* are very weakly expressed in the *Arabidopsis* stem. Within the *OSCA* family, no clade-specific expression pattern emerges from these data. Whatever the tissue analyzed, the expression of some *AtOSCA* genes is higher than *Piezo* or *AtMCA1*. In particular, *AtOSCA1.3* and *AtOSCA3.1* are highly expressed. While *AtPiezo* shows a homogeneous expression profile in the different stem tissues, *AtOSCA 3.1*, *1.3* and *2.2* have particular expression patterns with a very high level in the endodermis and the differentiating vessel elements. Interestingly, *AtMCA1* is expressed more strongly in the differentiating vessel elements than in the endodermis, a tissue involved in graviperception, while recent studies showed a role of this channel in hypergravity [104].

In order to investigate whether these tissue-specific expression patterns are found in other plant species, we also performed data mining and visualization on expression data obtained by RNA-seq after cryodissection of stem sections at the level of phloem and differentiating xylem tissues in *Populus tremula* [129]. As in *Arabidopsis*, *PtPiezo1* shows a homogeneous expression pattern in the different tissues (Figure 6). No data were found for the *PtPiezo2* and *PtOSCA2.1* genes, and the level of *PtOSCA1.4* and *1.5* expression is very low compared to the other genes. Among the genes encoding MS channels, *PtMCA1* is the most strongly expressed in the regions of expanding xylem and secondary wall development, whereas *PtMCA2* is very weakly expressed in these same regions. As in *Arabidopsis*, in the *OSCA* multigene family, the *PtOSCA3.1* isoform has the highest level of expression in the stem, but with a lower level in xylem cells during secondary wall differentiation. In clade 2, the genes are homogeneously expressed in all tissues except *PtaOSCA2.5*, for which the expression level is very low during the secondary wall differentiation phase. Finally, heterogeneous expression profiles are observed within clade 1 of the *OSCA* family: isoforms *1.1* and *1.2* show a peak of expression in the secondary wall formation zone while isoforms *1.3* and *1.7* in the phloem and isoforms *1.8* and *1.7* are more strongly expressed in the expanding xylem. Similarly, a peak of expression is detected for *PtOSCA1.9* in mature xylem cells. Note that no cambium-specific expression profile is observed for any of these genes. This study reveals more disparate expression levels between genes in the xylem expansion zone in poplar. It is interesting to note that in *Arabidopsis*, some genes also have a very specific expression profile in the differentiating xylem vessels.
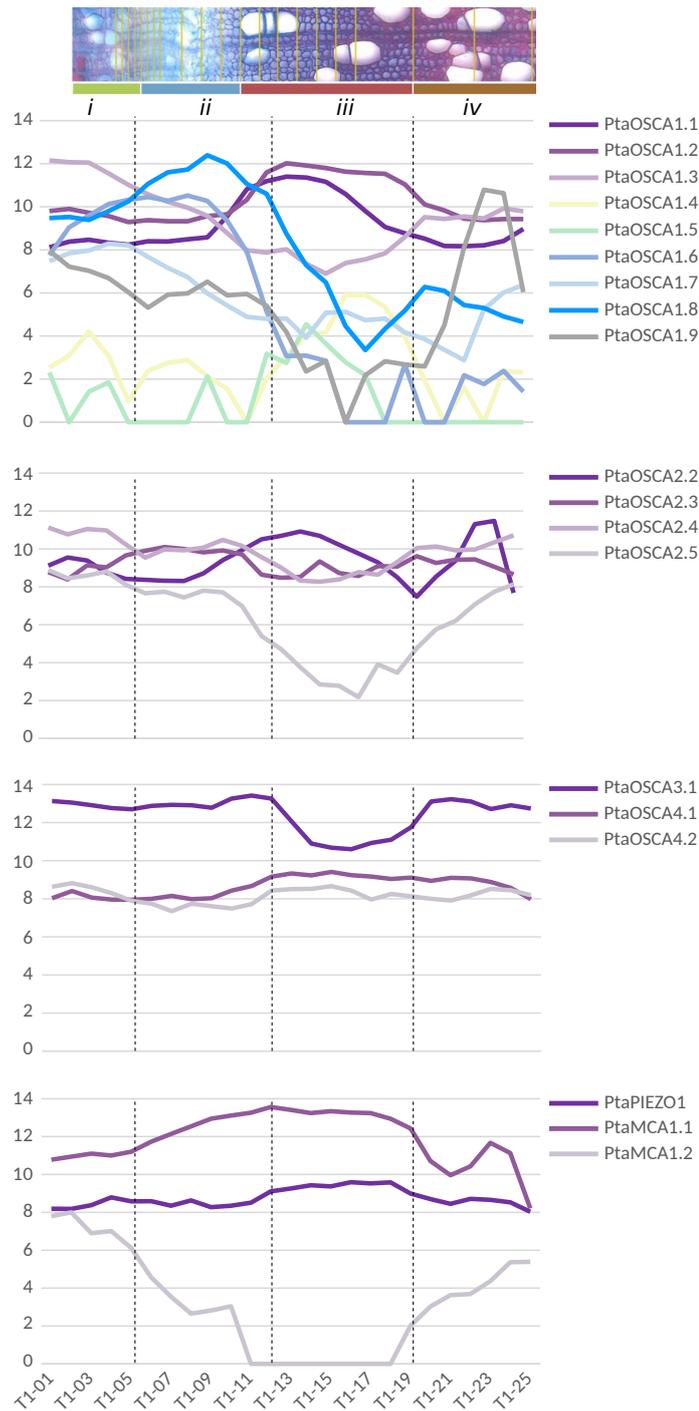
Figure 5. Expression patterns of *MCA*, *Piezo* and *OSCA* genes in different tissues of *Arabidopsis* mature inflorescence stem. Data were retrieved from the tissue-specific transcriptome study of the mature inflorescence stem of *Arabidopsis thaliana* [128] realized by analyzing mRNA from specifically labeled- nuclei covering a comprehensive set of distinct tissues (FANS/RNA-seq). Data are available at https://arabidopsis-stem.cos.uni-heidelberg.de. The values of expression levels (0 to 10,000) correspond to the mean of normalized read count values (by DESeq2). $n = 3$ for each population. * indicates a p-value < 0.01 in a Likelihood Ratio Test (LRT) results (by DESeq2) testing if genes have similar expression among the seven different tissues. See Appendix B.2 for details.

4. Conclusions

4.1. Unraveling the functions of mechanosensitive channels

Although major advances have been made in recent years demonstrating the essential role of mechanical stresses during a plant's life cycle, how cells perceive these signals and which signaling pathways trigger the physiological or developmental responses are questions that still require exciting research. While the dwarfing phenotype of *fer* loss-of-function mutants made it possible to establish the link between these proteins, cell growth and/or maintenance of cell wall integrity, no particular phenotype has been reported yet, for example, in the *piezo* loss-of-function mutants under normal growth conditions. More careful investigation, possibly under stressful conditions, could reveal the altered phenotype at either the macroscopic or molecular level. In this respect, the progress made in transcriptomic studies within a cell type opens new perspectives. Indeed, knowing in which tissue a MS channel gene is specifically expressed could allow a more specific targeting of the analysis of this tissue in KO-mutants to detect phenotypes. A further option could even be to modify the expression of the MS gene specifically in this tissue.

The creation of plants simultaneously mutated for several of these channels in the same tissue should also be tested to see if these proteins have redundant functions. This type of approach would be particularly interesting in the case of the multigenic *OSCA* family comprising a large number of genes. However, the immense number of possible combinations makes a systematic exploration of multiple mutants extremely laborious (for instance, there are 6188 possible quintuple KO-mutants with the 17 *OSCA* genes of *Populus trichocarpa*). Correlations in the tissue-specific expression of MS channel

Figure 6. Expression patterns of *MCA*, *Piezo* and *OSCA* genes in the wood-forming tissues of a wild-growing aspen genotype (*Populus tremula*). Data were retrieved from Sundell *et al*. ([129]; Supplementary Dataset 2). Pooled longitudinal tangential cryosections were used to obtain a continuous sequence of samples extending from differentiated phloem to mature xylem, with values of expression levels ranging from 0 to 16 (see Appendix B.3 for details). To better illustrate the location of the different tangential cryosections pooled to produce an RNA-seq sample, we showed the transverse cross-section image from the sampled tree T1 from [129, Figure 1]. The pooled samples are visualized by overlaying them on the transverse cross section and are grouped into four clusters (from *i* to *iv*). These clusters separate key reprogramming events represented by the dashed lines: (*i/ii*) occurs between phloem and xylem differentiation, in the middle of the dividing cambial cells; (*ii/iii*) marks the end of cell expansion and the onset of secondary cell wall formation; (*iii/iv*) marks the end of secondary cell wall deposition and the late maturation of xylem cells The cambium zone is located in cryosections T1-04, T1-05 and T1-06.

genes could be used as criteria to narrow down the candidates and focus on the most promising combinations.

Finally, the respective importance of these channels during mechanosensing would require the ability to correlate their activation with the magnitude of membrane tension. In this context, pioneer studies using fluorescent nano-probe reporter of membrane tension are very promising [133].

4.2. Transcriptional regulation of mechanosensitive channel genes following a mechanical stress

In addition to the tissue-specific expressions shown here, the transcriptional regulation of the MS channel genes has been poorly studied. Some results suggest that mechanical stress stimulates the transcription of these genes. For examples, Mousavi *et al.* [111] showed that *Arabidopsis thaliana* seedlings grown inside the Murashige and Skoog medium show a threefold higher expression of *AtPiezo* in the upper root and root cap than seedlings grown on the top of this medium. Zhang *et al.* [113] observed that the inoculation of a virus led to a significant increase in the expression of *AtPiezo* in petioles. In the carnivorous plant Venus flytrap, a transcriptomic study revealed that two *MSL* genes and an *OSCA* gene are upregulated in the touch-sensitive trigger hair following touch [126]. *Arabidopsis thaliana* seedlings under hypergravity conditions show upregulation of *AtMCA1* and *AtMCA2* in the hypocotyl compared to seedlings under the 1 g condition [104]. Since those mechanics-related gene expression patterns can suggest a gene function in the mecanosensing pathways, it could be interesting to reproduce our data-mining approach on previous transcriptome data obtained after a mechanical stress such as those performed after a transient stem/shoot bending [132,134], after a load has been placed on a tree stem [135] or after touching rosette leaves [136]. The expression dynamics of MS channel genes would probably give precious insight into their role in the physiological response, in short and long term. This kind of approach, combining mining and visualization of large molecular datasets with mechanical analyses at the tissue level, is a good illustration of the flourishing field of quantitative plant biology [137].

If the transcriptional regulation of MS channel genes after mechanical stress is to be confirmed, what are the implications for the amount of these proteins in the membranes? Is the transcriptional regulation just a way to maintain a constant concentration of MS channels, or could it modulate the mechanosensitivity of stimulated tissues?

4.3. Practical applications of thigmomorphogenesis

The ability of plants to respond to mechanical stress is more than a theoretical curiosity. For centuries, Japanese farmers have taken advantage of this phenomenon in a practice called "mugi-fumi", which consists in treading young wheat or barley plants to reduce the risk of lodging and increase yield [138]. This practical application of thigmomorphogenesis *avant la lettre* is bound to generalize and diversify as environmentally-friendly substitutes for current chemical treatments. For instance, mechanostimulating garden roses under greenhouse conditions increases branching and compactness [139], and could become an alternative to hormonal treatments in horticulture. In Poaceae, exposure to wind and imposed flexure have an impact on agronomic traits [140]. Furthermore, as several studies showed that various forms of mechanical stimuli enhanced plants' basal defense responses (see [141] for a review), mechanostimulation could be a potential priming method for sustainable agriculture, alternative to chemical-based priming. Developing efficient applications requires new phenotyping techniques for measuring mechanical traits such as the resistance to lodging [142], but also a deeper understanding of the actors involved in the mechanosensing pathways.

The relevance of thigmomorphogenesis to tree growth in non-controlled conditions [60] also opens new avenues for forest management, especially given the current increase in frequency of extreme windstorms [143]. At the macroscopic level, the functional biomechanical traits quantifying the strength and safety of trees against wind and self-buckling are well-established [144]. Trees acclimate to their mechanical environment by constantly adjusting these traits thanks to mechanosensing. However, the molecular actors involved in this feedback loop are largely unknown. Indeed, while many molecular studies have focused on the outermost tissues of organs (root cap, epidermis of the shoot apical meristem), few studies targeted the xylem, phloem or endodermis of stems, even though some of the MS channels genes are highly expressed in these tissues. The difficulty of performing *in vivo* spatio-temporal analyses in secondary tissues partly explains this lack of data. A future

solution could be experimental setups for growing cambium *in vitro*, mimicking the mechanical and hormonal environment of the cambium in trees. In any case, perennial plants are the systems in which investigating the localization and functions of MS channels is the most ecologically relevant.

Appendix A. Phylogeny

Coding sequences for *Piezo*, *MCA* and *OSCA* families were isolated using TBLASTX searches (Phytozome v12.1), in which *Arabidopsis thaliana* family members were used as query sequences against the coding sequences of *Populus trichocarpa* V3.0. Sequence alignments were generated using MAFFT version 7 with auto-option [145]. Maximum-likelihood trees were reconstructed from translated protein sequences using MEGA with LG substitution model. Bootstrapping with 1,000 replicates was performed to evaluate the credibility of tree topology. *MCA* and *OSCA* unrooted trees were obtained. The *Piezo* unrooted tree was obtained without bootstrap because it contained only 3 sequences.

The three illustrations of the tree of life in Figure 2 were based on the taxonomy of the National Center for Biotechnology Information, with simplifications for the sake of clarity.

Appendix B. Tissue-specific expression data

Appendix B.1. Data from single-cell RNA-seq of tissue/cell-types from Arabidopsis *roots*

Biological data were retrieved from a single-cell RNA-sequencing (scRNA-seq) experiment performed by Ryu *et al*. [127] from protoplasts of more than 10,000 *Arabidopsis* root cells issued of 5 days-old seedlings primary root tips. ScRNA-seq was performed using a commercially available droplet-based microfluidics. The authors obtained a total of 7,522 single-cell transcriptomes from three biological replicates of protoplasts from wild-type (Columbia ecotype) *Arabidopsis* root tips. Approximately 75,000 reads were obtained per cell, which generated a median of 24,000 unique molecular identifiers per cell, 5,000 expressed genes per cell, and more than 22,000 total genes detected in the population. An unsupervised clustering performed on using Seurat yielded nine major clusters of cell transcriptomes. To enable tissue/cell type assignment to particular clusters, the authors used the analysis of differentially expressed genes, gene ontology and the analysis of transcript accumulation of 86 marker genes known to be preferentially expressed in particular root tissue/cell types. Each dataset was log-normalized, scaled, and corrected for dataset-specific batch effects using ComBat (sva v3.26.00; [146]). In their article, the authors represent usually their data by plotting the single-cell transcriptomes via t-distributed stochastic neighbor embedding (tSNE) projection. This yielded largely overlapping distributions of cells from each of the biological replicates, indicating a high degree of reproducibility.

For the construction of our Figures 4 and B.1, the data for each gene were retrieved from the BAR ePlantArabidospsis website available at https://bar.utoronto.ca/eplant. For example, to retrieve
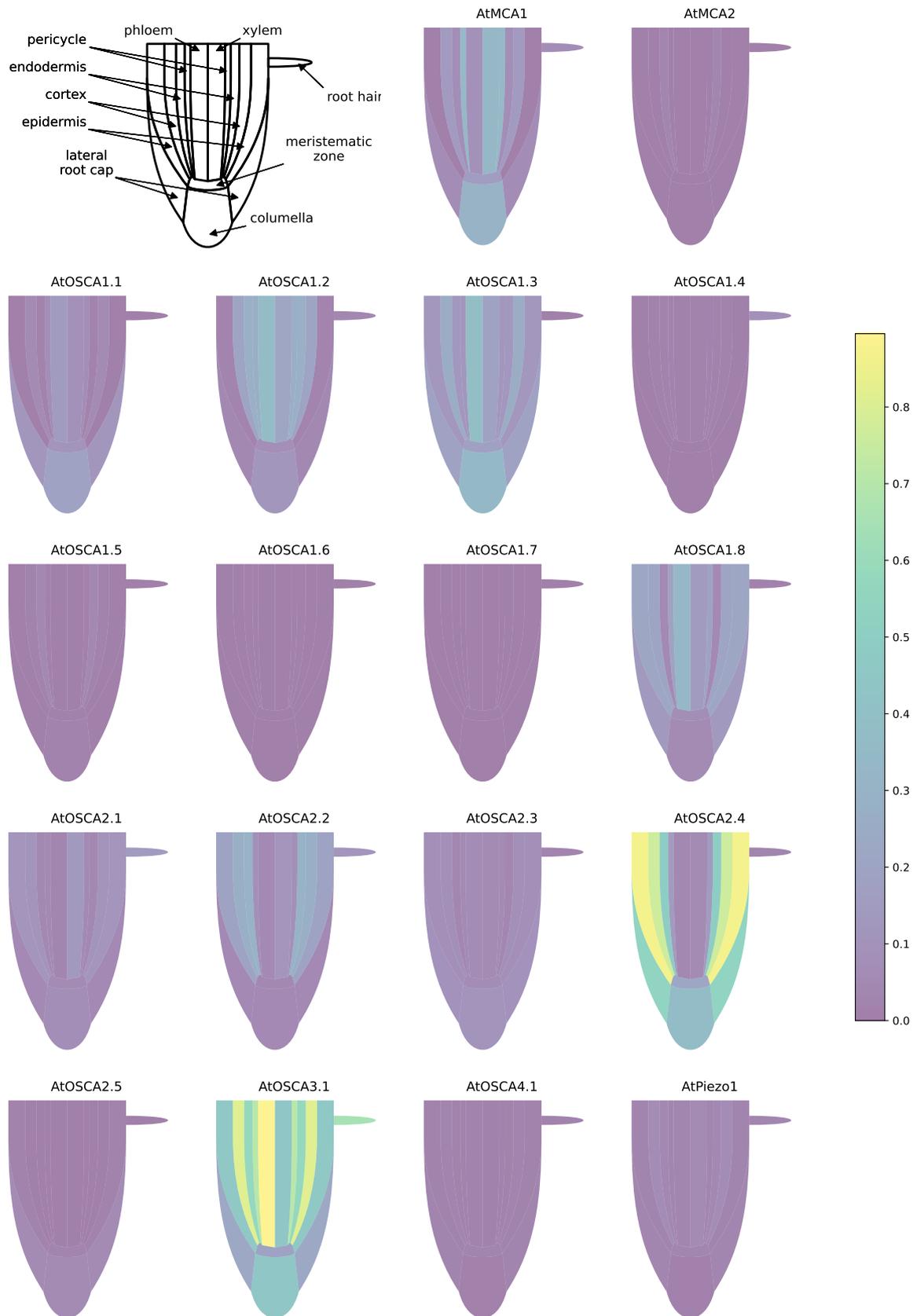
Figure A1. Expression patterns of *MCA*, *Piezo* and *OSCA* genes in different tissues of the *Arabidopsis* root using a common scale. Unlike Figure 4, which shows an individual scale for each gene, this figure allows comparisons between expression levels of different genes.

data for *AtOSCA1.1*, we entered its accession number AT4G04340 in the search bar (see Table S1 for the relationships between gene names and accession numbers), then clicked on *Tissue & Experiment eFP viewers*, then on *Single Cell eFP (RNA-Seq data)*. The resulting view can be accessed directly from the URL https://bar.utoronto.ca/eplant/?ActiveSpecies=Arabidopsis%20thaliana&Genes=AT4G043 40&ActiveGene=AT4G04340&ActiveView=SingleCellView. The raw data were then downloaded as JSON files.

For the different tissue/cell types, to facilitate the graphical representation of expression levels in tissues, only expression values from sub-clusters containing differentiated (not differentiating) cells were used. In the stele, only the expression data from xylem- and phloem-cell types are shown. In the meristematic zone, we represented the expression mean of dividing cells and cells from the quiescent center.

Appendix B.2. RNA-seq experiments from nuclei of different cell-types in mature inflorescence stem of Arabidopsis thaliana

To distinguish between the different cell types in mature inflorescence stems of *Arabidopsis*, Shi *et al* [128] produced transgenic *Arabidospsis* plants transformed with construction containing tissue-specific promoters controlling the expression of the GFP fluorescent reporter. The different promoter chosen by the authors were: the *NAC SECONDARY WALL THICKENING PROMOTING3 (NST3)* promoter to label fibers; the *VASCULAR-RELATED NAC DOMAIN PROTEIN7 (VND7)* promoter for differentiating vessel elements; the *PHLOEM INTERCALATED WITH XYLEM (PXY)/TDIF RECEP-TOR (TDR)* promoter for differentiating xylem cells and proximal cambium cells; the *SMAX1-LIKE5 (SMXL5)* promoter for differentiating phloem cells and distal cambium cells; the *ALTERED PHLOEM DEVELOPMENT (APL)* promoter for differentiated phloem cells; the *SCARECROW (SCR)* promoter for starch sheath cells; and the *LIPID TRANSFER PROTEIN1 (LTP1)* promoter for epidermis cells. The nuclei were isolated from the second internodes of *Arabidopsis* inflorescence stems. By combining fluorescence-activated nucleus sorting and laser-capture microdissection with next-generation RNA sequencing, the authors characterized and classified more than 15,000 genes as being differentially expressed in xylem vessels, fibers, the proximal and distal cambium, phloem, phloem cap, pith, starch sheath, and epidermis cells.

To prepare the spider-graphs in Figure 5, tissue-specific gene expression values were retrieved from https://arabidopsis-stem.cos.uni-heidelberg.de by successively entering the accession numbers of MS genes into the search bar. We computed the average expression levels of the three biological replicates.

Appendix B.3. RNA-seq experiments from cryosections spanning the secondary phloem, vascular cambium, and wood-forming tissues of Populus tremula

Biological data were retrieved from the RNA-seq experiment performed by Sundell *et al*. [129, Supplementary Dataset 2] and also available on the interactive web resource http://aspwood.popgenie.org. In this study, the authors collected and cut longitudinal tangential cryosections (15 μm thick) using a cryo-microtome in the stem zone covering the entire current-year radial growth zone of a poplar trees. The total number of sections varied from 105 to 135 in the four different 45-year old aspen trees sampled during the middle of the growing season. For RNA-seq experiments, these sections were pooled into 25 to 28 samples for each replicate tree, thanks to images taken with a light microscope during the process of sectioning. The pooling was based on the estimated tissue composition from anatomical inspection. Details of the composition of the 25 samples are given in [129, Supplementary Dataset 1]. After RNA-seq, the values of expression levels were estimated after normalization of the read counts using a variance-stabilizing transformation as implemented in DESeq [129].

To prepare the Figure 6, we retrieved data directly from the Supplementary Dataset 2 of [129], which is a Microsoft Excell file. To simplify the illustration of expression profiles (the number of sections composing the 4 clusters can be separated from several sections between the 4 tree replicates), we showed only the results obtained on the sampled tree T1 since similar expression profiles are obtained when the three other samples trees are analyzed. By a hierarchical clustering from mRNA expression values for all expressed genes, Sundell *et al*. [129] identified four sample clusters of expression. The authors describe that these gene expression clusters were found to separate key reprogramming events:

(*i/ii*) occurs between phloem and xylem differentiation, in the middle of the dividing cambial cells; (*ii/iii*) marks the end of cell expansion and the onset of secondary cell wall formation; (*iii/iv*) marks the end of secondary cell wall deposition and the late maturation of xylem cells.

References

1. Moulia, B.; Coutand, C.; Julien, J.L. Mechanosensitive control of plant growth: Bearing the load, sensing, transducing and responding. *Frontiers in Plant Science* **2015**, *6*. doi:10.3389/fpls.2015.00052.
2. Gardiner, B.; Berry, P.; Moulia, B. Review: Wind impacts on plant growth, mechanics and damage. *Plant Science* **2016**, *245*, 94 – 118. doi:10.1016/j.plantsci.2016.01.006.
3. Alméras, T.; Gril, J.; Costes, E. Bending of apricot-tree branches under the weight of axillary productions: confrontation of a mechanical model to experimental data. *Trees* **2002**, *16*, 5–15. doi:10.1007/s00468-001-0139-1.
4. Moulia, B.; Bastien, R.; Chauvet-Thiry, H.; Leblanc-Fournier, N. Posture control in land plants: growth, position sensing, proprioception, balance, and elasticity. *Journal of Experimental Botany* **2019**, *70*, 3467–3494. doi:10.1093/jxb/erz278.
5. Kolb, E.; Legué, V.; Bogeat-Triboulot, M.B. Physical root-soil interactions. *Physical Biology* **2017**, *14*, 065004. doi:10.1088/1478-3975/aa90dd.
6. Puijalon, S.; Bouma, T.J.; Douady, C.J.; van Groenendael, J.; Anten, N.P.R.; Martel, E.; Bornette, G. Plant resistance to mechanical stress: evidence of an avoidance–tolerance trade-off. *New Phytologist* **2011**, *191*, 1141–1149. doi:10.1111/j.1469-8137.2011.03763.x.
7. Denny, M.; Gaylord, B. The mechanics of wave-swept algae. *Journal of Experimental Biology* **2002**, *205*, 1355–1362.
8. Green, P.B. Mechanism for plant cellular morphogenesis. *Science* **1962**, *138*, 1404–1405. doi:10.1126/science.138.3548.1404.
9. Lockhart, J.A. An analysis of irreversible plant cell elongation. *Journal of Theoretical Biology* **1965**, *8*, 264–275. doi:10.1016/0022-5193(65)90077-9.
10. Weber, A.; Braybrook, S.; Huflejt, M.; Mosca, G.; Routier-Kierzkowska, A.L.; Smith, R.S. Measuring the mechanical properties of plant cells by combining micro-indentation with osmotic treatments. *Journal of Experimental Botany* **2015**, *66*, 3229–3241. doi:10.1093/jxb/erv135.
11. Mosca, G.; Sapala, A.; Strauss, S.; Routier-Kierzkowska, A.L.; Smith, R.S. On the micro-indentation of plant cells in a tissue context. *Physical Biology* **2017**, *14*, 015003. doi:10.1088/1478-3975/aa5698.
12. Sampathkumar, A.; Krupinski, P.; Wightman, R.; Milani, P.; Berquand, A.; Boudaoud, A.; Hamant, O.; Jönsson, H.; Meyerowitz, E.M. Subcellular and supracellular mechanical stress prescribes cytoskeleton behavior in *Arabidopsis* cotyledon pavement cells. *eLife* **2014**, *3*, e01967. doi:10.7554/eLife.01967.
13. Sapala, A.; Runions, A.; Routier-Kierzkowska, A.L.; Gupta, M.D.; Hong, L.; Hofhuis, H.; Verger, S.; Mosca, G.; Li, C.B.; Hay, A.; others. Why plants make puzzle cells, and how their shape emerges. *eLife* **2018**, *7*, e32794. doi:10.7554/eLife.32794.
14. Kierzkowski, D.; Routier-Kierzkowska, A.L. Cellular basis of growth in plants: geometry matters. *Current Opinion in Plant Biology* **2019**, *47*, 56–63. Growth and development, doi:10.1016/j.pbi.2018.09.008.
15. Long, Y.; Cheddadi, I.; Mosca, G.; Mirabet, V.; Dumond, M.; Kiss, A.; Traas, J.; Godin, C.; Boudaoud, A. Cellular heterogeneity in pressure and growth emerges from tissue topology and geometry. *Current Biology* **2020**, *30*, 1504 – 1516.e8. doi:10.1016/j.cub.2020.02.027.
16. Verger, S.; Long, Y.; Boudaoud, A.; Hamant, O. A tension-adhesion feedback loop in plant epidermis. *eLife* **2018**, *7*, e34460. doi:10.7554/eLife.34460.
17. Hejnowicz, Z. Graviresponses in herbs and trees: a major role for the redistribution of tissue and growth stresses. *Planta* **1997**, *203*, S136–S146. doi:10.1007/PL00008102.
18. Vandiver, R.; Goriely, A. Tissue tension and axial growth of cylindrical structures in plants and elastic tissues. *EPL (Europhysics Letters)* **2008**, *84*, 58004. doi:10.1209/0295-5075/84/58004.
19. Moulia, B.; Fournier, M. The power and control of gravitropic movements in plants: a biomechanical and systems biology view. *Journal of Experimental Botany* **2009**, *60*, 461–486. doi:10.1093/jxb/ern341.
20. Moulia, B. Plant biomechanics and mechanobiology are convergent paths to flourishing interdisciplinary research. *Journal of Experimental Botany* **2013**, *64*, 4617–4633. doi:10.1093/jxb/ert320.
21. Kierzkowski, D.; Nakayama, N.; Routier-Kierzkowska, A.L.; Weber, A.; Bayer, E.; Schorderet, M.; Reinhardt, D.; Kuhlemeier, C.; Smith, R.S. Elastic domains regulate growth and organogenesis in the plant shoot apical meristem. *Science* **2012**, *335*, 1096–1099. doi:10.1126/science.1213100.
22. Hamant, O.; Heisler, M.G.; Jönsson, H.; Krupinski, P.; Uyttewaal, M.; Bokov, P.; Corson, F.; Sahlin, P.; Boudaoud, A.; Meyerowitz, E.M.; Couder, Y.; Traas, J. Developmental patterning by mechanical signals in *Arabidopsis*. *Science* **2008**, *322*, 1650–1655. doi:10.1126/science.1165594.
23. Beauzamy, L.; Louveaux, M.; Hamant, O.; Boudaoud, A. Mechanically, the shoot apical meristem of *Arabidopsis* behaves like a shell inflated by a pressure of about 1 MPa. *Frontiers in Plant Science* **2015**, *6*, 1038. doi:10.3389/fpls.2015.01038.
24. Hejnowicz, Z.; Sievers, A. Tissue stresses in organs of herbaceous plants: II. Determination in three dimensions in the hypocotyl of sunflower. *Journal of Experimental Botany* **1995**, *46*, 1045–1053. doi:10.1093/jxb/46.8.1045.
25. Kutschera, U.; Niklas, K.J. The epidermal-growth-control theory of stem elongation: An old and a new perspective. *Journal of Plant Physiology* **2007**, *164*, 1395–1409. doi:10.1016/j.jplph.2007.08.002.
26. Archer, R.R. *Growth stresses and strains in trees*; Springer: Berlin, 1987.

27. Alméras, T.; Clair, B. Critical review on the mechanisms of maturation stress generation in trees. *Journal of The Royal Society Interface* **2016**, *13*, 20160550. doi:10.1098/rsif.2016.0550.

28. Alméras, T.; Fournier, M. Biomechanical design and long-term stability of trees: Morphological and wood traits involved in the balance between weight increase and the gravitropic reaction. *Journal of Theoretical Biology* **2009**, *256*, 370–381. doi:10.1016/j.jtbi.2008.10.011.

29. Clair, B.; Ghislain, B.; Prunier, J.; Lehnebach, R.; Beauchêne, J.; Alméras, T. Mechanical contribution of secondary phloem to postural control in trees: the bark side of the force. *New Phytologist* **2018**, *0*. doi:10.1111/nph.15375.

30. Telewski, F.W. A unified hypothesis of mechanoperception in plants. *American Journal of Botany* **2006**, *93*, 1466–1476. doi:10.3732/ajb.93.10.1466.

31. Bidhendi, A.J.; Altartouri, B.; Gosselin, F.P.; Geitmann, A. Mechanical stress initiates and sustains the morphogenesis of wavy leaf epidermal cells. *Cell Reports* **2019**, *28*, 1237–1250.e6. doi:10.1016/j.celrep.2019.07.006.

32. Reinhardt, D.; Pesce, E.R.; Stieger, P.; Mandel, T.; Baltensperger, K.; Bennett, M.; Traas, J.; Friml, J.; Kuhlemeier, C. Regulation of phyllotaxis by polar auxin transport. *Nature* **2003**, *426*, 255–260. doi:10.1038/nature02081.

33. Smith, R.S.; Guyomarc'h, S.; Mandel, T.; Reinhardt, D.; Kuhlemeier, C.; Prusinkiewicz, P. A plausible model of phyllotaxis. *Proceedings of the National academy of Sciences of the United States of America* **2006**, *103*, 1301–6. doi:10.1073/pnas.0510457103.

34. Bayer, E.M.; Smith, R.S.; Mandel, T.; Nakayama, N.; Sauer, M.; Prusinkiewicz, P.; Kuhlemeier, C. Integration of transport-based models for phyllotaxis and midvein formation. *Genes & Development* **2009**, *23*, 373–384. doi:10.1101/gad.497009.

35. Hartmann, F.P.; Barbier de Reuille, P.; Kuhlemeier, C. Toward a 3D model of phyllotaxis based on a biochemically plausible auxin-transport mechanism. *PLOS Computational Biology* **2019**, *15*, 1–21. doi:10.1371/journal.pcbi.1006896.

36. Arsuffi, G.; Braybrook, S.A. Acid growth: an ongoing trip. *Journal of Experimental Botany* **2018**, *69*, 137–146. doi:10.1093/jxb/erx390.

37. Heisler, M.G.; Hamant, O.; Krupinski, P.; Uyttewaal, M.; Ohno, C.; Jönsson, H.; Traas, J.; Meyerowitz, E.M. Alignment between PIN1 polarity and microtubule orientation in the shoot apical meristem reveals a tight coupling between morphogenesis and auxin transport. *PLoS Biology* **2010**, *8*, e1000516. doi:10.1371/journal.pbio.1000516.

38. Nakayama, N.; Smith, R.; Mandel, T.; Robinson, S.; Kimura, S.; Boudaoud, A.; Kuhlemeier, C. Mechanical regulation of auxin-mediated growth. *Current Biology* **2012**, *22*, 1468–1476. doi:https://doi.org/10.1016/j.cub.2012.06.050.

39. Landrein, B.; Kiss, A.; Sassi, M.; Chauvet, A.; Das, P.; Cortizo, M.; Laufs, P.; Takeda, S.; Aida, M.; Traas, J.; Vernoux, T.; Boudaoud, A.; Hamant, O. Mechanical stress contributes to the expression of the *STM* homeobox gene in *Arabidopsis* shoot meristems. *eLife* **2015**, *4*, e07811. doi:10.7554/eLife.07811.

40. Hejnowicz, Z.; Rusin, A.; Rusin, T. Tensile tissue stress affects the orientation of cortical microtubules in the epidermis of sunflower hypocotyl. *Journal of plant growth regulation* **2000**, *19*, 31–44. doi:10.1007/s003440000005.

41. Robinson, S.; Kuhlemeier, C. Global compression reorients cortical microtubules in *Arabidopsis* hypocotyl epidermis and promotes growth. *Current Biology* **2018**, *28*, 1794 – 1802.e2. doi:https://doi.org/10.1016/j.cub.2018.04.028.

42. Burian, A.; Ludynia, M.; Uyttewaal, M.; Traas, J.; Boudaoud, A.; Hamant, O.; Kwiatkowska, D. A correlative microscopy approach relates microtubule behaviour, local organ geometry, and cell growth at the *Arabidopsis* shoot apical meristem. *Journal of Experimental Botany* **2013**, *64*, 5753–5767. doi:10.1093/jxb/ert352.

43. Hamant, O.; Moulia, B. How do plants read their own shapes? *New Phytologist* **2016**, *212*, 333–337. 2016-21674, doi:10.1111/nph.14143.

44. Kabir, A.M.R.; Inoue, D.; Hamano, Y.; Mayama, H.; Sada, K.; Kakugo, A. Biomolecular motor modulates mechanical property of microtubule. *Biomacromolecules* **2014**, *15*, 1797–1805. doi:10.1021/bm5001789.

45. Mirabet, V.; Krupinski, P.; Hamant, O.; Meyerowitz, E.M.; Jönsson, H.; Boudaoud, A. The self-organization of plant microtubules inside the cell volume yields their cortical localization, stable alignment, and sensitivity to external cues. *PLOS Computational Biology* **2018**, *14*, 1–23. doi:10.1371/journal.pcbi.1006011.

46. Hamant, O.; Inoue, D.; Bouchez, D.; Dumais, J.; Mjolsness, E. Are microtubules tension sensors? *Nature communications* **2019**, *10*, 1–12. doi:10.1038/s41467-019-10207-y.

47. Paredez, A.R.; Somerville, C.R.; Ehrhardt, D.W. Visualization of cellulose synthase demonstrates functional association with microtubules. *Science* **2006**, *312*, 1491–1495. doi:10.1126/science.1126551.

48. Hervieux, N.; Dumond, M.; Sapala, A.; Routier-Kierzkowska, A.L.; Kierzkowski, D.; Roeder, A.; Smith, R.; Boudaoud, A.; Hamant, O. A mechanical feedback restricts sepal growth and shape in *Arabidopsis*. *Current Biology* **2016**, *26*, 1019 – 1028. doi:https://doi.org/10.1016/j.cub.2016.03.004.

49. Hervieux, N.; Tsugawa, S.; Fruleux, A.; Dumond, M.; Routier-Kierzkowska, A.L.; Komatsuzaki, T.; Boudaoud, A.; Larkin, J.C.; Smith, R.S.; Li, C.B.; Hamant, O. Mechanical shielding of rapidly growing cells buffers growth heterogeneity and contributes to organ shape reproducibility. *Current Biology* **2017**, *27*, 3468 – 3479.e4. doi:10.1016/j.cub.2017.10.033.

50. Stokes, A.; Nicoll, B.C.; Coutts, M.P.; Fitter, A.H. Responses of young Sitka spruce clones to mechanical perturbation and nutrition: effects on biomass allocation, root development, and resistance to bending. *Canadian Journal of Forest Research* **1997**, *27*, 1049–1057. doi:10.1139/x97-041.

51. Nicoll, B.C.; Gardiner, B.A.; Peace, A.J. Improvements in anchorage provided by the acclimation of forest trees to wind stress. *Forestry: An International Journal of Forest Research* **2008**, *81*, 389–398. doi:10.1093/forestry/cpn021.

52. Telewski, F.W.; Pruyn, M.L. Thigmomorphogenesis: a dose response to flexing in *Ulmus americana* seedlings. *Tree Physiology* **1998**, *18*, 65–68. doi:10.1093/treephys/18.1.65.

53. Coutand, C.; Dupraz, C.; Jaouen, G.; Ploquin, S.; Adam, B. Mechanical stimuli regulate the allocation of biomass in trees: Demonstration with young *Prunus avium* trees. *Annals of Botany* **2008**, *101*, 1421–1432. doi:10.1093/aob/mcn054.

54. Niez, B.; Dlouhá, J.; Moulia, B.; Badel, E. Water-stressed or not, the mechanical acclimation is a priority requirement for trees. *Trees* **2019**, *33*, 279–291. doi:10.1007/s00468-018-1776-y.

55. Telewski, F.W. Structure and function of flexure wood in *Abies fraseri*. *Tree Physiology* **1989**, *5*, 113–121. doi:10.1093/treephys.

56. Roignant, J.; Badel, É.; Leblanc-Fournier, N.; Brunel-Michac, N.; Ruelle, J.; Moulia, B.; Decourteix, M. Feeling stretched or compressed? The multiple mechanosensitive responses of wood formation to bending. *Annals of Botany* **2018**, *121*, 1151–1161. doi:10.1093/aob/mcx211.

57. Niez, B.; Dlouhá, J.; Gril, J.; Ruelle, J.; Toussaint, E.; Moulia, B.; Badel, E. Mechanical properties of "flexure wood": compressive stresses in living trees improve the mechanical resilience of wood and its resistance to damage. *Annals of Forest Science* **2020**, *77*, 17. doi:10.1007/s13595-020-0926-8.

58. Jaffe, M.J. Thigmomorphogenesis: The response of plant growth and development to mechanical stimulation. *Planta* **1973**, *114*, 143–157. doi:10.1007/BF00387472.

59. Fournier, M.; Stokes, A.; Coutand, C.; Fourcaud, T.; Moulia, B. Tree biomechanics and growth strategies in the context of forest functional ecology. In *Ecology and biomechanics: A mechanical approach to the ecology of animals and plants*; Press, C., Ed.; CRC Press, 2006; pp. 1–34.

60. Bonnesoeur, V.; Constant, T.; Moulia, B.; Fournier, M. Forest trees filter chronic wind-signals to acclimate to high winds. *New Phytologist* **2016**, *210*, 850–860. doi:10.1111/nph.13836.

61. Paul-Victor, C.; Rowe, N. Effect of mechanical perturbation on the biomechanics, primary growth and secondary tissue development of inflorescence stems of *Arabidopsis thaliana*. *Annals of Botany* **2010**, *107*, 209–218. doi:10.1093/aob/mcq227.

62. Zhdanov, O.; Blatt, M.R.; Zare-Behtash, H.; Busse, A. Wind-evoked anemotropism affects the morphology and mechanical properties of *Arabidopsis*. *Journal of Experimental Botany* **2021**, *72*, 1906–1918. eraa541, doi:10.1093/jxb/eraa541.

63. Anten, N.P.R.; Alcalá-Herrera, R.; Schieving, F.; Onoda, Y. Wind and mechanical stimuli differentially affect leaf traits in Plantago major. *New Phytologist* **2010**, *188*, 554–564. doi:10.1111/j.1469-8137.2010.03379.x.

64. Schoelynck, J.; Puijalon, S.; Meire, P.; Struyf, E. Thigmomorphogenetic responses of an aquatic macrophyte to hydrodynamic stress. *Frontiers in Plant Science* **2015**, *6*, 43. doi:10.3389/fpls.2015.00043.

65. Ditengou, F.A.; Teale, W.D.; Kochersperger, P.; Flittner, K.A.; Kneuper, I.; van der Graaff, E.; Nziengui, H.; Pinosa, F.; Li, X.; Nitschke, R.; Laux, T.; Palme, K. Mechanical induction of lateral root initiation in *Arabidopsis thaliana*. *Proceedings of the National Academy of Sciences* **2008**, *105*, 18818–18823. doi:10.1073/pnas.0807814105.

66. Richter, G.L.; Monshausen, G.B.; Krol, A.; Gilroy, S. Mechanical stimuli modulate lateral root organogenesis. *Plant Physiology* **2009**, *151*, 1855–1866. doi:10.1104/pp.109.142448.

67. Monshausen, G.B.; Bibikova, T.N.; Weisenseel, M.H.; Gilroy, S. Ca2+ regulates reactive oxygen species production and pH during mechanosensing in *Arabidopsis* roots. *The Plant Cell* **2009**, *21*, 2341–2356. doi:10.1105/tpc.109.068395.

68. Bizet, F.; Bengough, A.G.; Hummel, I.; Bogeat-Triboulot, M.B.; Dupuy, L.X. 3D deformation field in growing plant roots reveals both mechanical and biological responses to axial mechanical forces. *Journal of Experimental Botany* **2016**, *67*, 5605–5614. doi:10.1093/jxb/erw320.

69. Roué, J.; Chauvet, H.; Brunel-Michac, N.; Bizet, F.; Moulia, B.; Badel, E.; Legué, V. Root cap size and shape influence responses to the physical strength of the growth medium in *Arabidopsis thaliana* primary roots. *Journal of Experimental Botany* **2020**, *71*, 126–137. doi:10.1093/jxb/erz418.

70. Coutand, C.; Julien, J.; Moulia, B.; Mauget, J.; Guitard, D. Biomechanical study of the effect of a controlled bending on tomato stem elongation: global mechanical analysis. *Journal of Experimental Botany* **2000**, *51*, 1813–1824. doi:10.1093/jexbot/51.352.1813.

71. Moulia, B.; Der Loughian, C.; Bastien, R.; Martin, O.; Rodríguez, M.; Gourcilleau, D.; Barbacci, A.; Badel, E.; Franchel, J.; Lenne, C.; Roeckel-Drevet, P.; Allain, J.M.; Frachisse, J.M.; de Langre, E.; Coutand, C.; Fournier-Leblanc, N.; Julien, J.L. Integrative mechanobiology of growth and architectural development in changing mechanical environments. In *Mechanical Integration of Plant Cells and Plants*; Wojtaszek, P., Ed.; Springer Berlin Heidelberg, 2011; Vol. 9, *Signaling and Communication in Plants*, pp. 269–302. doi:10.1007/978-3-642-19091-9_11.

72. Lopez, R.; Badel, É.; Peraudeau, S.; Leblanc-Fournier, N.; Beaujard, F.; Julien, J.L.; Cochard, H.; Moulia, B. Tree shoot bending generates hydraulic pressure pulses: a new long-distance signal? *Journal of Experimental Botany* **2014**, *65*, 1997–2008. doi:10.1093/jxb/eru045.

73. Louf, J.F.; Guéna, G.; Badel, E.; Forterre, Y. Universal poroelastic mechanism for hydraulic signals in biomimetic and natural branches. *Proceedings of the National Academy of Sciences* **2017**, *114*, 11034–11039. doi:10.1073/pnas.1707675114.

74. Tinturier, E.; Badel, E.; Leblanc-Fournier, N.; Julien, J.L. Stem bending generates electrical response in poplar. *Physiologia Plantarum* **2021**, *n/a*. doi:10.1111/ppl.13494.

75. Chauvin, A.; Caldelari, D.; Wolfender, J.L.; Farmer, E.E. Four 13-lipoxygenases contribute to rapid jasmonate synthesis in wounded *Arabidopsis thaliana* leaves: A role for lipoxygenase 6 in responses to long-distance wound signals. *New Phytologist* **2013**, *197*, 566–575. doi:10.1111/nph.12029.

76. Chehab, E.; Yao, C.; Henderson, Z.; Kim, S.; Braam, J. *Arabidopsis* touch-induced morphogenesis is jasmonate mediated and protects against pests. *Current Biology* **2012**, *22*, 701–706. doi:10.1016/j.cub.2012.02.061.

77. Farmer, E.E.; Gasperini, D.; Acosta, I.F. The squeeze cell hypothesis for the activation of jasmonate synthesis in response to wounding. *New Phytologist* **2014**, *204*, 282–288. doi:10.1111/nph.12897.

78. Tixier, A.; Badel, E.; Franchel, J.; Lakhal, W.; Leblanc-Fournier, N.; Moulia, B.; Julien, J.L. Growth and molecular responses to long-distance stimuli in poplars: Bending vs flame wounding. *Physiologia Plantarum* **2014**, *150*, 225–237. doi:10.1111/ppl.12089.

79. Fal, K.; Korsbo, N.; Alonso-Serra, J.; Teles, J.; Liu, M.; Refahi, Y.; Chabouté, M.E.; Jönsson, H.; Hamant, O. Tissue folding at the organ-meristem boundary results in nuclear compression and chromatin compaction. *Proceedings of the National Academy of Sciences* **2021**, *118*. doi:10.1073/pnas.2017859118.

80. Bacete, L.; Hamann, T. The role of mechanoperception in plant cell wall integrity maintenance. *Plants* **2020**, *9*, 574. doi:10.3390/plants9050574.

81. Frachisse, J.M.; Thomine, S.; Allain, J.M. Calcium and plasma membrane force-gated ion channels behind development. *Current Opinion in Plant Biology* **2020**, *53*, 57–64. Growth and development, doi:10.1016/j.pbi.2019.10.006.

82. Guo, H.; Li, L.; Ye, H.; Yu, X.; Algreen, A.; Yin, Y. Three related receptor-like kinases are required for optimal cell elongation in *Arabidopsis thaliana*. *Proceedings of the National Academy of Sciences of the United States of America* **2009**, *106*, 7648–7653. doi:10.1073/pnas.0812346106.

83. Shih, H.W.; Miller, N.D.; Dai, C.; Spalding, E.P.; Monshausen, G.B. The receptor-like kinase FERONIA is required for mechanical signal transduction in *Arabidopsis* seedlings. *Current Biology* **2014**, *24*, 1887–1892. doi:10.1016/j.cub.2014.06.064.

84. Li, E.; Wang, G.; Zhang, Y.; Kong, Z.; Li, S. FERONIA mediates root nutating growth. *The Plant Journal* **2020**, *104*, 1105–1116. doi:10.1111/tpj.14984.

85. Dong, Q.; Zhang, Z.; Liu, Y.; Tao, L.; Liu, H. FERONIA regulates auxin-mediated lateral root development and primary root gravitropism. *FEBS Letters* **2019**, *593*, 97–106. doi:10.1002/1873-3468.13292.

86. Wang, K.; Yang, Z.; Qing, D.; Ren, F.; Liu, S.; Zheng, Q.; Liu, J.; Zhang, W.; Dai, C.; Wu, M.; Chehab, E.W.; Braam, J.; Li, N. Quantitative and functional posttranslational modification proteomics reveals that TREPH1 plays a role in plant touch-delayed bolting. *Proceedings of the National Academy of Sciences of the United States of America* **2018**, *115*, E10265–E10274. doi:10.1073/pnas.1814006115.

87. Hamilton, E.S.; Schlegel, A.M.; Haswell, E.S. United in diversity: Mechanosensitive ion channels in plants. *Annual Review of Plant Biology* **2015**, *66*, 113–137. doi:10.1146/annurev-arplant-043014-114700.

88. Basu, D.; Haswell, E.S. Plant mechanosensitive ion channels: an ocean of possibilities, 2017. doi:10.1016/j.pbi.2017.07.002.

89. White, P.J.; Broadley, M.R. Calcium in plants. *Annals of Botany* **2003**, *92*, 487–511. doi:10.1093/aob/mcg164.

90. Knight, M.R.; Smith, S.M.; Trewavas, A.J. Wind-induced plant motion immediately increases cytosolic calcium. *Proceedings of the National Academy of Sciences of the United States of America* **1992**, *89*, 4967–4971. doi:10.1073/pnas.89.11.4967.

91. Legué, V.; Blancaflor, E.; Wymer, C.; Perbal, G.; Fantin, D.; Gilroy, S. Cytoplasmic free Ca2+ in *Arabidopsis* roots changes in response to touch but not gravity. *Plant Physiology* **1997**, *114*, 789–800. doi:10.1104/pp.114.3.789.

92. Kurusu, T.; Kuchitsu, K.; Nakano, M.; Nakayama, Y.; Iida, H. Plant mechanosensing and Ca2+ transport. *Trends in Plant Science* **2013**, *18*, 227–233. doi:10.1016/j.tplants.2012.12.002.

93. Monshausen, G.B.; Haswell, E.S. A force of nature: Molecular mechanisms of mechanoperception in plants, 2013. doi:10.1093/jxb/ert204.

94. Fromm, J.; Lautner, S. Electrical signals and their physiological significance in plants. *Plant, Cell & Environment* **2007**, *30*, 249–257. doi:10.1111/j.1365-3040.2006.01614.x.

95. Choi, W.G.; Hilleary, R.; Swanson, S.J.; Kim, S.H.; Gilroy, S. Rapid, long-distance electrical and calcium signaling in plants. *Annual Review of Plant Biology* **2016**, *67*, 287–307. doi:10.1146/annurev-arplant-043015-112130.

96. Braam, J.; Davis, R.W. Rain-, wind-, and touch-induced expression of calmodulin and calmodulin-related genes in *Arabidopsis*. *Cell* **1990**, *60*, 357–364. doi:10.1016/0092-8674(90)90587-5.

97. Nakagawa, Y.; Katagiri, T.; Shinozaki, K.; Qi, Z.; Tatsumi, H.; Furuichi, T.; Kishigami, A.; Sokabe, M.; Kojima, I.; Sato, S.; Kato, T.; Tabata, S.; Iida, K.; Terashima, A.; Nakano, M.; Ikeda, M.; Yamanaka, T.; Iida, H. Arabidopsis plasma membrane protein crucial for Ca2+ influx and touch sensing in roots. *Proceedings of the National Academy of Sciences of the United States of America* **2007**, *104*, 3639–3644. doi:10.1073/pnas.0607703104.

98. Nakano, M.; Iida, K.; Nyunoya, H.; Iida, H. Determination of structural regions important for Ca2+ uptake activity in *Arabidopsis* MCA1 and MCA2 expressed in yeast. *Plant and Cell Physiology* **2011**, *52*, 1915–1930. doi:10.1093/pcp/pcr131.

99. Shigematsu, H.; Iida, K.; Nakano, M.; Chaudhuri, P.; Iida, H.; Nagayama, K. Structural characterization of the mechanosensitive channel candidate MCA2 from *Arabidopsis thaliana*. *PLoS ONE* **2014**, *9*, e87724. doi:10.1371/journal.pone.0087724.

100. Kamano, S.; Kume, S.; Iida, K.; Lei, K.J.; Nakano, M.; Nakayama, Y.; Iida, H. Transmembrane topologies of Ca2+-permeable mechanosensitive channels MCA1 and MCA2 in *Arabidopsis thaliana*. *Journal of Biological Chemistry* **2015**, *290*, 30901–30909. doi:10.1074/jbc.M115.692574.

101. Nishii, K.; Möller, M.; Iida, H. Mix and match: Patchwork domain evolution of the land plant-specific Ca2+-permeable mechanosensitive channel MCA. *PLOS ONE* **2021**, *16*, e0249735. doi:10.1371/journal.pone.0249735.

102. Furuichi, T.; Iida, H.; Sokabe, M.; Tatsumi, H. Expression of *Arabidopsis* MCA1 enhanced mechanosensitive channel activity in the *Xenopus laevis* oocyte plasma membrane. *Plant Signaling & Behavior* **2012**, *7*, 1022–1026. doi:10.4161/psb.20783.

103. Yamanaka, T.; Nakagawa, Y.; Mori, K.; Nakano, M.; Imamura, T.; Kataoka, H.; Terashima, A.; Iida, K.; Kojima, I.; Katagiri, T.; Shinozaki, K.; Iida, H. MCA1 and MCA2 that mediate Ca2+ uptake have distinct and overlapping roles in *Arabidopsis*. *Plant Physiology* **2010**, *152*, 1284–1296. doi:10.1104/pp.109.147371.

104. Hattori, T.; Otomi, Y.; Nakajima, Y.; Soga, K.; Wakabayashi, K.; Iida, H.; Hoson, T. MCA1 and MCA2 are involved in the response to hypergravity in *Arabidopsis* hypocotyls. *Plants* **2020**, *9*, 590. doi:10.3390/plants9050590.

105. Coste, B.; Mathur, J.; Schmidt, M.; Earley, T.J.; Ranade, S.; Petrus, M.J.; Dubin, A.E.; Patapoutian, A. Piezo1 and Piezo2 are essential components of distinct mechanically activated cation channels. *Science* **2010**, *330*, 55–60. doi:10.1126/science.1193270.

106. Guo, Y.R.; MacKinnon, R. Structure-based membrane dome mechanism for piezo mechanosensitivity. *eLife* **2017**, *6*. doi:10.7554/eLife.33660.

107. Saotome, K.; Murthy, S.E.; Kefauver, J.M.; Whitwam, T.; Patapoutian, A.; Ward, A.B. Structure of the mechanically activated ion channel Piezo1. *Nature* **2018**, *554*, 481–486. doi:10.1038/nature25453.

108. Zhao, Q.; Zhou, H.; Chi, S.; Wang, Y.; Wang, J.; Geng, J.; Wu, K.; Liu, W.; Zhang, T.; Dong, M.Q.; Wang, J.; Li, X.; Xiao, B. Structure and mechanogating mechanism of the Piezo1 channel. *Nature* **2018**, *554*, 487–492.

109. Wang, Y.; Xiao, B. The mechanosensitive Piezo1 channel: structural features and molecular bases underlying its ion permeation and mechanotransduction. *The Journal of Physiology* **2018**, *596*, 969–978. doi:10.1113/JP274404.

110. Fang, X.Z.; Zhou, T.; Xu, J.Q.; Wang, Y.X.; Sun, M.M.; He, Y.J.; Pan, S.W.; Xiong, W.; Peng, Z.K.; Gao, X.H.; Shang, Y. Structure, kinetic properties and biological function of mechanosensitive Piezo channels. *Cell and Bioscience* **2021**, *11*, 1–20. doi:10.1186/s13578-020-00522-z.

111. Mousavi, S.A.R.; Dubin, A.E.; Zeng, W.Z.; Coombs, A.M.; Do, K.; Ghadiri, D.A.; Keenan, W.T.; Ge, C.; Zhao, Y.; Patapoutian, A. PIEZO ion channel is required for root mechanotransduction in *Arabidopsis thaliana*. *Proceedings of the National Academy of Sciences* **2021**, *118*. doi:10.1073/pnas.2102188118.

112. Wu, J.; Lewis, A.H.; Grandl, J. Touch, tension, and transduction–the function and regulation of Piezo ion channels. *Trends in biochemical sciences* **2017**, *42*, 57–71. doi:10.1016/j.tibs.2016.09.004.

113. Zhang, Z.; Tong, X.; Liu, S.Y.; Chai, L.X.; Zhu, F.F.; Zhang, X.P.; Zou, J.Z.; Wang, X.B. Genetic analysis of a Piezo-like protein suppressing systemic movement of plant viruses in *Arabidopsis thaliana*. *Scientific Reports* **2019**, *9*, 3187. doi:10.1038/s41598-019-39436-3.

114. Fang, X.; Liu, B.; Shao, Q.; Huang, X.; Li, J.; Luan, S.; He, K. Atpiezo plays an important role in root cap mechanotransduction. *International Journal of Molecular Sciences* **2021**, *22*, 1–13. doi:10.3390/ijms22010467.

115. Radin, I.; Richardson, R.A.; Coomey, J.H.; Weiner, E.R.; Bascom, C.S.; Li, T.; Bezanilla, M.; Haswell, E.S. Plant PIEZO homologs modulate vacuole morphology during tip growth. *Science* **2021**, *373*, 586–590. doi:10.1126/science.abe6310.

116. Dünser, K.; Gupta, S.; Herger, A.; Feraru, M.I.; Ringli, C.; Kleine-Vehn, J. Extracellular matrix sensing by FERONIA and Leucine-Rich Repeat Extensins controls vacuolar expansion during cellular elongation in *Arabidopsis thaliana*. *The EMBO Journal* **2019**, *38*, e100353. doi:https://doi.org/10.15252/embj.2018100353.

117. Hou, C.; Tian, W.; Kleist, T.; He, K.; Garcia, V.; Bai, F.; Hao, Y.; Luan, S.; Li, L. DUF221 proteins are a family of osmosensitive calcium-permeable cation channels conserved across eukaryotes. *Cell Research* **2014**, *24*, 632–635. doi:10.1038/cr.2014.14.

118. Murthy, S.E.; Dubin, A.E.; Whitwam, T.; Jojoa-Cruz, S.; Cahalan, S.M.; Mousavi, S.A.R.; Ward, A.B.; Patapoutian, A. OSCA/TMEM63 are an evolutionarily conserved family of mechanically activated ion channels. *eLife* **2018**, *7*. doi:10.7554/eLife.41844.

119. Jojoa-Cruz, S.; Saotome, K.; Murthy, S.E.; Tsui, C.C.A.; Sansom, M.S.; Patapoutian, A.; Ward, A.B. Cryo-EM structure of the mechanically activated ion channel OSCA1.2. *eLife* **2018**, *7*. doi:10.7554/eLife.41845.

120. Liu, X.; Wang, J.; Sun, L. Structure of the hyperosmolality-gated calcium-permeable channel OSCA1.2. *Nature Communications* **2018**, *9*, 1–9. doi:10.1038/s41467-018-07564-5.

121. Zhang, M.; Wang, D.; Kang, Y.; Wu, J.X.; Yao, F.; Pan, C.; Yan, Z.; Song, C.; Chen, L. Structure of the mechanosensitive OSCA channels. *Nature Structural & Molecular Biology* **2018**, *25*, 850–858. doi:10.1038/s41594-018-0117-6.

122. Maity, K.; Heumann, J.M.; McGrath, A.P.; Kopcho, N.J.; Hsu, P.K.; Lee, C.W.; Mapes, J.H.; Garza, D.; Krishnan, S.; Morgan, G.P.; Hendargo, K.J.; Klose, T.; Rees, S.D.; Medrano-Soto, A.; Saier, M.H.; Piñeros, M.; Komives, E.A.; Schroeder, J.I.; Chang, G.; Stowell, M.H.B. Cryo-EM structure of OSCA1.2 from *Oryza sativa* elucidates the mechanical basis of potential membrane hyperosmolality gating. *Proceedings of the National Academy of Sciences* **2019**, *116*, 14309–14318. doi:10.1073/pnas.1900774116.

123. Yuan, F.; Yang, H.; Xue, Y.; Kong, D.; Ye, R.; Li, C.; Zhang, J.; Theprungsirikul, L.; Shrift, T.; Krichilsky, B.; Johnson, D.M.; Swift, G.B.; He, Y.; Siedow, J.N.; Pei, Z.M. OSCA1 mediates osmotic-stress-evoked Ca2+ increases vital for osmosensing in *Arabidopsis*. *Nature* **2014**, *514*, 367–371. doi:10.1038/nature13593.

124. Thor, K.; Jiang, S.; Michard, E.; George, J.; Scherzer, S.; Huang, S.; Dindas, J.; Derbyshire, P.; Leitão, N.; DeFalco, T.A.; Köster, P.; Hunter, K.; Kimura, S.; Gronnier, J.; Stransfeld, L.; Kadota, Y.; Bücherl, C.A.; Charpentier, M.; Wrzaczek, M.; MacLean, D.; Oldroyd, G.E.; Menke, F.L.; Roelfsema, M.R.G.; Hedrich, R.; Feijó, J.; Zipfel, C. The calcium-permeable channel OSCA1.3 regulates plant stomatal immunity. *Nature* **2020**, *585*, 569–573. doi:10.1038/s41586-020-2702-1.

125. Cao, L.; Zhang, P.; Lu, X.; Wang, G.; Wang, Z.; Zhang, Q.; Zhang, X.; Wei, X.; Mei, F.; Wei, L.; Wang, T. Systematic analysis of the maize *OSCA* genes revealing *ZmOSCA* family members involved in osmotic stress and *ZmOSCA2.4* confers enhanced drought tolerance in transgenic arabidopsis. *International Journal of Molecular Sciences* **2020**, *21*, 351. doi:10.3390/ijms21010351.

126. Procko, C.; Murthy, S.; Keenan, W.T.; Mousavi, S.A.R.; Dabi, T.; Coombs, A.; Procko, E.; Baird, L.; Patapoutian, A.; Chory, J. Stretch-activated ion channels identified in the touch-sensitive structures of carnivorous droseraceae plants. *eLife* **2021**, *10*. doi:10.7554/eLife.64250.

127. Ryu, K.H.; Huang, L.; Kang, H.M.; Schiefelbein, J. Single-cell RNA sequencing resolves molecular relationships among individual plant cells. *Plant Physiology* **2019**, *179*, 1444–1456. doi:10.1104/pp.18.01482.

128. Shi, D.; Jouannet, V.; Agustí, J.; Kaul, V.; Levitsky, V.; Sanchez, P.; Mironova, V.V.; Greb, T. Tissue-specific transcriptome profiling of the *Arabidopsis* inflorescence stem reveals local cellular signatures. *The Plant Cell* **2021**, *33*, 200–223. doi:10.1093/plcell/koaa019.

129. Sundell, D.; Street, N.R.; Kumar, M.; Mellerowicz, E.J.; Kucukoglu, M.; Johnsson, C.; Kumar, V.; Mannapperuma, C.; Delhomme, N.; Nilsson, O.; Tuominen, H.; Pesquet, E.; Fischer, U.; Niittylä, T.; Sundberg, B.; Hvidsten, T.R. Aspwood: High-spatial-resolution transcriptome profiles reveal uncharacterized modularity of wood formation in populus tremula. *Plant Cell* **2017**, *29*, 1585–1604. doi:10.1105/tpc.17.00153.

130. Jacobsen, A.G.; Jervis, G.; Xu, J.; Topping, J.F.; Lindsey, K. Root growth responses to mechanical impedance are regulated by a network of ROS, ethylene and auxin signalling in *Arabidopsis*. *New Phytologist* **2021**, *231*, 225–242. doi:10.1111/nph.17180.

131. Lee, H.J.; Kim, H.S.; Park, J.M.; Cho, H.S.; Jeon, J.H. PIN-mediated polar auxin transport facilitates root-obstacle avoidance. *New Phytologist* **2020**, *225*, 1285–1296. doi:10.1111/nph.16076.

132. Pomiès, L.; Decourteix, M.; Franchel, J.; Moulia, B.; Leblanc-Fournier, N. Poplar stem transcriptome is massively remodelled in response to single or repeated mechanical stimuli. *BMC Genomics* **2017**, *18*, 300.

133. Colom, A.; Derivery, E.; Soleimanpour, S.; Tomba, C.; Molin, M.D.; Sakai, N.; González-Gaitán, M.; Matile, S.; Roux, A. A fluorescent membrane tension probe. *Nature Chemistry* **2018**, *10*, 1118–1125. doi:10.1038/s41557-018-0127-3.

134. Xing, L.; Zhang, D.; Qi, S.; Chen, X.; An, N.; Li, Y.; Zhao, C.; Han, M.; Zhao, J. Transcription profiles reveal the regulatory mechanisms of spur bud changes and flower induction in response to shoot bending in apple (*Malus domestica* Borkh.). *Plant Molecular Biology* **2019**, *99*, 45–66. doi:10.1007/s11103-018-0801-2.

135. Alonso-Serra, J.; Safronov, O.; Lim, K.J.; Fraser-Miller, S.J.; Blokhina, O.B.; Campilho, A.; Chong, S.L.; Fagerstedt, K.; Haavikko, R.; Helariutta, Y.; Immanen, J.; Kangasjärvi, J.; Kauppila, T.J.; Lehtonen, M.; Ragni, L.; Rajaraman, S.; Räsänen, R.M.; Safdari, P.; Tenkanen, M.; Yli-Kauhaluoma, J.T.; Teeri, T.H.; Strachan, C.J.; Nieminen, K.; Salojärvi, J. Tissue-specific study across the stem reveals the chemistry and transcriptome dynamics of birch bark. *New Phytologist* **2019**, *222*, 1816–1831. doi:10.1111/nph.15725.

136. Lee, D.; Polisensky, D.H.; Braam, J. Genome-wide identification of touch- and darkness-regulated *Arabidopsis* genes: a focus on calmodulin-like and *XTH* genes. *New Phytologist* **2005**, *165*, 429–444. doi:10.1111/j.1469-8137.2004.01238.x.

137. Autran, D.; Bassel, G.W.; Chae, E.; Ezer, D.; Ferjani, A.; Fleck, C.; Hamant, O.; Hartmann, F.P.; Jiao, Y.; Johnston, I.G.; Kwiatkowska, D.; Lim, B.L.; Mahönen, A.P.; Morris, R.J.; Mulder, B.M.; Nakayama, N.; Sozzani, R.; Strader, L.C.; ten Tusscher, K.; Ueda, M.; Wolf, S. What is quantitative plant biology? *Quantitative Plant Biology* **2021**, *2*, e10. doi:10.1017/qpb.2021.8.

138. Iida, H. Mugifumi, a beneficial farm work of adding mechanical stress by treading to wheat and barley seedlings. *Frontiers in Plant Science* **2014**, *5*, 453. doi:10.3389/fpls.2014.00453.

139. Morel, P.; Crespel, L.; Galopin, G.; Moulia, B. Effect of mechanical stimulation on the growth and branching of garden rose. *Scientia Horticulturae* **2012**, *135*, 59–64. doi:10.1016/j.scienta.2011.12.007.

140. Gladala-Kostarz, A.; Doonan, J.H.; Bosch, M. Mechanical stimulation in *Brachypodium distachyon*: Implications for fitness, productivity, and cell wall properties. *Plant, Cell & Environment* **2020**, *43*, 1314–1330. doi:https://doi.org/10.1111/pce.13724.

141. Ghosh, R.; Barbacci, A.; Leblanc-Fournier, N. Mechanostimulation: a promising alternative for sustainable agriculture practices. *Journal of Experimental Botany* **2021**, *72*, 2877–2888. doi:10.1093/jxb/erab036.

142. de Langre, E.; Penalver, O.; Hémon, P.; Frachisse, J.M.; Bogeat-Triboulot, M.B.; Niez, B.; Badel, É.; Moulia, B. Nondestructive and fast vibration phenotyping of plants. *Plant Phenomics* **2019**, *2019*, 6379693. doi:10.34133/2019/6379693.

143. Hawcroft, M.; Walsh, E.; Hodges, K.; Zappa, G. Significantly increased extreme precipitation expected in Europe and North America from extratropical cyclones. *Environmental Research Letters* **2018**, *13*, 124006. doi:10.1088/1748-9326/aaed59.

144. Fournier, M.; Dlouhá, J.; Jaouen, G.; Alméras, T. Integrative biomechanics for tree ecology: beyond wood density and strength. *Journal of Experimental Botany* **2013**, *64*, 4793–4815. doi:10.1093/jxb/ert279.

145. Katoh, K.; Rozewicki, J.; Yamada, K.D. MAFFT online service: multiple sequence alignment, interactive sequence choice and visualization. *Briefings in Bioinformatics* **2017**, *20*, 1160–1166. doi:10.1093/bib/bbx108.

146. Leek, J.T.; Johnson, W.E.; Parker, H.S.; Jaffe, A.E.; Storey, J.D. The sva package for removing batch effects and other unwanted variation in high-throughput experiments. *Bioinformatics* **2012**, *28*, 882–883. doi:10.1093/bioinformatics/bts034.

Species	Gene name	Accession number	Sequence Source
Arabidopsis thaliana	AtOSCA1.1	AT4G04340.1	TAIR10, Phytozome
	AtOSCA1.2	AT4G22120.1	
	AtOSCA1.3	AT1G11960.1	
	AtOSCA1.4	AT1G62320.1	
	AtOSCA1.5	AT3G21620.1	
	AtOSCA1.6	AT4G15430.1	
	AtOSCA1.7	AT4G02900.1	
	AtOSCA1.8	AT1G32090.1	
	AtOSCA2.1	AT1G58520.1	
	AtOSCA2.2	AT1G10090.1	
	AtOSCA2.3	AT3G01100.1	
	AtOSCA2.4	AT1G69450.1	
	AtOSCA2.5	AT3G54510.1	
	AtOSCA3.1	AT1G30360.1	
	AtOSCA4.1	AT4G35870.1	
	AtMCA1	AT4G35920.1	
	AtMCA2	AT2G17780.1	
	AtPiezo1	AT2G48060.1	
Populus trichocarpa	PtOSCA1.1	Potri.004G005900	V3.1, Phytozome
	PtOSCA1.2	Potri.004G006000	
	PtOSCA1.3	Potri.011G009900	
	PtOSCA1.4	Potri.004G006100	
	PtOSCA1.5	Potri.011G009800	
	PtOSCA1.6	Potri.002G226800	
	PtOSCA1.7	Potri.014G156100	
	PtOSCA1.8	Potri.001G133800	
	PtOSCA1.9	Potri.003G099800	
	PtOSCA2.1	Potri.003G200900	
	PtOSCA2.2	Potri.002G113800	
	PtOSCA2.3	Potri.004G115800	
	PtOSCA2.4	Potri.008G091200	
	PtOSCA2.5	Potri.010G164100	
	PtOSCA3.1	Potri.001G358300	
	PtOSCA4.1	Potri.005G108600	
	PtOSCA4.2	Potri.007G063700	
	PtMCA1	Potri.005G110000	
	PtMCA2	Potri.010G184700	
	PtPiezo1	Potri.014G137200	
	PtPiezo2	Potri.005G037700	